Opportunistic Photoplethysmography in Mobile Fingerprint Authentication

（モバイルデバイスでの指紋認証時に
指尖容積脈波を同時に取得する手法の研究）

37-166491 Takahiro Hashizume （橋爪崇弘）

Supervisor: Koji Yatani（矢谷浩司）

Department of Electrical Engineering and Information Systems
Graduate School of Engineering
The University of Tokyo

This thesis is submitted for the degree of
Master of Engineering

January 31st, 2018

Acknowledgements

I would like to express my deepest gratitude to my supervisor, Prof. Koji Yatani, whose comments and suggestions were of inestimable value for my master thesis. Through weekly 1-on-1 meetings, he had given me many chances to discuss not only my research but also my career vision, which have guided me to the best direction. I strongly believe that he is the best boss ever!

I would like to offer my special thanks to Prof. Yoshihiro Kawahara, who kindly gave me a permission to use their facilities. I would also like to extend my thanks to Koya Narumi and Takuya Sasatani for their great help in my research life. They have always given me much help and worked hard together since I was in Kawahara laboratory. I would not have enjoyed my research life without their generous support!

The members in Interactive Intelligent Systems Laboratory have also contributed to my research. Special thanks go to Namiki Shimoo and Takuma Yoshitani, who have gone through 2-year research life together. The advice given by Takuya Arizono has been a great help in analyzing data and developing the sensing algorithm. Assistance provided by Daisuke Shibato was also greatly appreciated. I am particularly grateful for the assistance given by Misako Motooka, who had kindly provided me support for much paperwork. I want to thank all the experiment participants in my user evaluation, who willingly shared their time for me.

Lastly, I would like to express the deepest appreciation to my family and Aoi Nishiha for their moral support and warm encouragement.

Abstract

Recent commodity smartphones have biometric sensing capabilities, allowing their daily use for authentication and identification. This increasing use of biometric systems motivates me to design an opportunistic way to sense user's additional physiological or behavioral data. I define this concurrent physiological or behavioral data sensing during biometric authentication or identification as *dual-purpose biometrics*. As an instance of *dual-purpose biometrics*, I develop photoplethysmography (PPG) sensing during mobile fingerprint authentication, called Auth 'n' Scan. My system opportunistically extracts cardiovascular information, such as a heart rate and its variability, while users perform phone unlock of a smartphone. To achieve this sensing, my Auth 'n' Scan system attaches four PPG units around a fingerprint sensor. The system also performs noise removal and signal selection to accurately estimate cardiovascular information. My system evaluations with 10 participants show that despite a little low precision (a standard deviation of 3–7), estimation of heart rates with high accuracy (under a mean error of 1) is possible from PPG data of five seconds and longer if their baseline information is given. This thesis first introduces the background of my research, discusses the definition of *dual-purpose biometrics*, and describes my research contributions. It then presents my literature survey related to this research. In chapter 3–5, this thesis presents a principle of PPG, the implementation of hardware and signal processing algorithm, and my system evaluation. I also report the results of my system evaluations including the heart-related features estimation and user-interview results. I discuss the feasibility of opportunistic PPG sensing in mobile fingerprint authentication, and conclude with future research directions.

概要

スマートデバイスの普及により生体認証は日常的に使用できる技術となっている．生体認証においては認証に必要な情報だけではなく，ユーザの健康に関する情報も同時に取得できる可能性がある．このような生体認証と同時にユーザの生理学的あるいは行動に関するデータを取得するシステムを Dual-purpose biometrics と本研究では定義する．本論文では，Dual-purpose biometrics の一例として，指紋認証と同時に指尖容積脈波を取得するシステム Auth 'n' Scan を提案し，そのハードウェア・アルゴリズム開発とユーザ評価を行った．このシステムはユーザがスマートフォンで指紋認証を行う際に，同時にその指から心拍数や心拍変動などの心臓に関する情報を取得する．これを実現するため，Auth 'n' Scan はスマートフォンの指紋認証センサの周囲に複数の指尖容積脈波センサと回路機構を備えている．Auth 'n' Scan はこれら複数のセンサから取得した信号からノイズを除去し，最も信頼できるチャネルを選定した後，心臓に関する情報を推定する．10 人の実験参加者に対してユーザ評価を行なった結果，ユーザの平常時心拍数を利用し，かつ 5 秒以上信号を取得できれば高い精度（平均誤差 1 未満）で心拍数を推定できることがわかった．本論文ではまず研究背景と Dual-purpose biometrics の定義，そして本研究が行なった貢献について述べる．次に関連研究について詳しく述べ，本研究と既存研究の差異を明確化する．第 3 章から第 5 章においては PPG の原理，ハードウェアと信号処理アルゴリズムの実装，そして評価実験の手順について論じる．その後，評価実験で得られたデータを用いて，心臓に関する情報の推定結果やユーザスタディの結果について論じる．最後に指尖容積脈波を同時に取得する指紋認証システムの実現可能性と，今後の研究課題について議論する．

Table of contents

List of figures

List of tables

Chapter 1

Introduction

1.1 Background

Recent identification and authentication systems employ biometrics, physiological or behavior data that are distinctive among individuals. Such biometric authentication has become commodity in recent computer devices. For instance, it can allow smartphone users to unlock their devices with fingerprints, reducing the effort for entering codes or passwords. Prior work has also revealed that users positively received biometric authentication systems [6, 9]. A report claims that users who own smartphones with a fingerprint authentication capability unlock their devices 80 times a day through biometrics [5]. I believe that future ubiquitous and mobile systems would further integrate biometric authentication/identification, encouraging its use in a daily life.

This increasing use of biometric authentication motivates me to design an opportunistic way to sense user's additional physiological or behavioral data. For instance, when users unlock a smartphone, a system can sense physiological data (e.g., vital information, respiration or perspiration) besides fingerprints. Extracted data can benefit a wealth of applications, including life-logging, personal informatics, and healthcare monitoring. I define this concurrent physiological or behavioral data sensing during biometric authentication or identification as *dual-purpose biometrics*. Figure 1.1 illustrates a conceptual comparison between existing biometric authentication/identification systems and dual-purpose biometrics.

Dual-purpose biometrics can offer unique benefits to existing biometrics systems. Additional applications enabled by dual-purpose biometrics may encourage more use of biometric authentication/identification systems. As dual-purpose biometrics systems perform

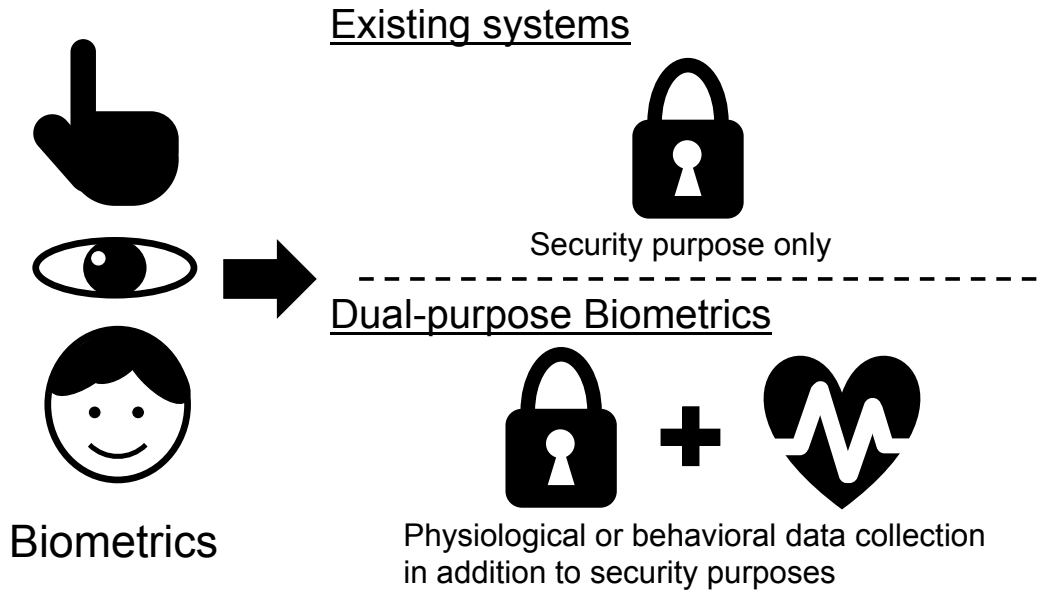

Fig. 1.1 A concept illustration of *dual-purpose biometrics*. Dual-purpose biometrics enables concurrent physiological or behavioral sensing during biometric authentication or identification. This sensing mechanism offers an opportunistic and unobtrusive way to acquire healthcare information as well as encourages the use of authentication/identification systems through additional applications enabled.

sensing during authentication or identification, users would not need to perform separate explicit data recording or wear additional devices. This may lead to improved compliance of data collection.

In this work, I demonstrate a system that senses user's cardiovascular data during fingerprint authentication on a smartphone as an instance of my dual-purpose biometrics concept. My system, called Auth 'n' Scan, utilizes custom-made hardware containing multiple photoplethysmography (PPG) sensors. I design them to surround the fingerprint sensor on a smartphone. In this manner, users can record their cardiovascular data during authentication[1], and do not need to perform separate explicit measurements. Because my system enables sensing at different times of the day, it can obtain information that otherwise is difficult to infer, such as heart rate changes due to the circadian rhythm [38] and distribution transition in a Poincaré plot (discussed in Section 6.3).

Besides the proposal of dual-purpose biometrics, the main objective of this work is to demonstrate the feasibility of concurrent sensing of fingerprints for authentication and

[1]In this work, I mainly refer to authentication scenarios though my concept and system can be applied for identification systems.

cardiovascular data for healthcare monitoring applications. When users place fingers for unlocking smartphones with their fingerprints for at least five seconds, my system extracts short-term cardiovascular features, such as a heart rate and its variability, with PPG sensors. In addition, the Auth 'n' Scan system reconstructs longer-term features (e.g., a feature in a Poincaré plot) from a series of fragmented measurements if the sensing duration of ten seconds is allowed. Although my current prototype needs at least five seconds of recording for accurate heart rate estimation, the majority of participants in my user study agreed that it is acceptable at the exchange of the benefit by Auth 'n' Scan.

1.2 Dual-purpose Biometrics

Auth 'n' Scan is an instance of *dual-purpose biometrics*, my security system concept proposal. Dual-purpose biometrics represents an identification or authentication system which simultaneously senses users' physiological or behavioral data for additional purposes, such as healthcare monitoring and life-logging (Figure 1.1). Users frequently engage in activities that require authentication in a daily life (e.g., unlocking a smartphone, opening an office's door, and placing an order in an online system). Various biometrics authentication systems become available in these scenarios. Dual-purpose biometrics exploits these increasing biometrics authentication interactions as sensing opportunities. In this work, I demonstrate cardiovascular sensing in mobile fingerprint authentication for phone unlock as an example of dual-purpose biometrics. Future work should explore a broader area of dual-purpose biometrics (e.g., skin moisture sensing in authentication with fingers or hands; heart rate sensing in face authentication; and throat disorder detection in voice-based authentication).

Dual-purpose biometrics aims to encourage the use of authentication systems by providing additional applications it enables. Sasse and Flechais discussed the role of security systems through the lens of human factor analysis [39]. In a goal-oriented process, there are two types of tasks: *production tasks* (tasks that are necessary to complete to achieve the goal) and *supporting tasks* (tasks that are not directly essential to achieve the goal but would provide value or useful functionality for a production task). This analysis can explain why users often circumvent or disable security systems. According to Sasse and Flechais' argument, security is a supporting task. Although security provides protection value, it does not directly contribute to a production task or offer merits immediately perceivable to users. Thus, security systems may become a burden, resulting in its abandonment. In dual-purpose biometrics

systems, authentication can become a production task for the other purposes. For example, a phone unlock would become an interaction to record heart rate information for a healthcare application. In this manner, users can obtain more direct benefits from security systems besides protection. I hope that dual-purpose biometrics would contribute to further persuasion and penetration of daily security system use.

Dual-purpose biometrics is also regarded as another form of unobtrusive sensing for daily healthcare monitoring. Some existing healthcare monitoring systems involve explicit measurements of physiological data or user activities (e.g., using a blood pressure monitor or making manual annotations upon smoking). Prior work has addressed this issue in the context of experience sampling [21]. Such measurement burden could also degrade user compliance and data reliability in healthcare monitoring applications. One possible solution is unobtrusive sensing, a technology which performs sensing while users are engaging in a main task [26]. Although unobtrusive sensing is promising to reduce user's burden, Korhonen et al. discussed the following three challenges: 1) a requirement for user identification; 2) limitations on continuous monitoring; and 3) constrained sensing capabilities of physiological data. My dual-purpose biometrics uniquely solves the first and third issues. As dual-purpose biometrics concurrently performs authentication and sensing, user identification can be immediately given under the user's permission. Upon biometric authentication, users are asked to steadily expose part of the body. A system thus has a sufficient opportunity to acquire various physiological data (e.g., cardiovascular information in the Auth 'n' Scan system). Dual-purpose biometrics broadens the field of unobtrusive sensing, and encourages further research in creative exploitation of biometric authentication.

Although it is beyond the scope of this work, dual-purpose biometrics can also contribute to multimodal biometrics [36]. Multimodal biometrics means using multiple physiological or behavioral traits to improve security robustness. Dual-purpose biometrics is different in enabling additional applications instead of reinforcing security. But future dual-purpose biometrics systems could offer unique security enhancement (e.g., ECG data can be another evidence for user authentication [37]).

1.3 Contributions

The contributions of this work are as follows:

My proposal of the dual-purpose biometrics concept

I introduce the concept of dual-purpose biometrics. As summarized in Figure 1.1, dual-purpose biometrics systems enable both authentication/identification and unobtrusive sensing for additional applications. This capability is beneficial for security systems (e.g., encouraging more use of them) as well as sensing (e.g., unobtrusively acquiring users' data).

Hardware for concurrent fingerprint and cardiovascular sensing on a smartphone

I develop custom hardware to attach four PPG units to the periphery of a fingerprint sensor on a smartphone. My informal evaluation confirms that my hardware design is robust to different finger placement and ambient light conditions.

Cardiovascular feature inference from short-term PPG data

My algorithm selects a signal among four PPG channels that can best describe cardiovascular information. It then extracts heart rates and peak-to-peak intervals from that signal. In addition, my algorithm attempts to reconstruct a Poincaré plot, comprised of pairs of two adjacent PPIs, from a set of fragmented measurements.

System and user evaluations of Auth 'n' Scan

I conducted system evaluations with 10 healthy adult participants. My results achieved accurate heart rate estimation from data in the duration of 5 seconds or longer if the baseline heart rate data of each participant is given. More specifically, the estimation error was within 1 and its standard deviation was between 3 and 7. In addition, I confirm that reconstruction of Poincaré plots is possible for some of my participants though a sufficient number of adjacent PPI pairs are necessary. My participants agreed that a 5-second sensing duration was acceptable because Auth 'n' Scan offers heart rate information.

Chapter 2

Related Work

2.1 Fingerprint Sensing Technology

A fingerprint is a pattern formed by friction ridges observed in epidermis. As fingerprint patterns are considered to be distinctive and immutable, they are widely used in authentication. Fingerprints can be found in several locations of a human body, such as a palm and foot, but those in fingertips are the most common part for security system use. Although prior work has studied various matching methods, a typical approach is to use feature points called minutiae [22]. Minutiae refer to ridge endings and bifurcations in a fingerprint pattern. A typical fingerprint image contains 20–70 minutiae points [22]. Based on the location and orientation of each minutiae, a matching algorithm calculates similarity between a given fingerprint and those in a database, and performs identification (i.e., determines who this user is) or authentication (i.e., judges whether this user is really the person who she claims to be) [35].

A broad range of fingerprint sensing approaches exists: optical, capacitive, RF-based (radio frequency), pressure-based, thermal, and ultrasonic sensors [34]. An RF-based method is considered to be the most accurate and reliable [42]. An RF fingerprint sensor consists of a 2D array of tiny antennas each of which produces reading of the depth of a point. Because of the ability to capture fingerprint images beneath the skin, the RF array-based fingerprint sensor technology is robust to different skin conditions, environments, and even minor finger surface contamination [42].

Since Apple integrated this type of sensors into iPhone 5S in 2013, fingerprint authentication on smartphones becomes common. De Luca et al. showed that one of the main

decision factors to enable biometrics on smartphones is its usability [9]. Another study reported that people prefer fingerprint authentication to face recognition or traditional password-based approaches for phone unlocking because of its usability [6]. According to Apple's report in 2016, 89% owners of iPhones and iPads with a fingerprint authentication capability regularly used the Touch ID service [5]. This report also showed that they unlocked their devices with Touch ID roughly 80 times a day on average. Recent research has demonstrated broader applications of mobile fingerprint authentication. Holz et al. developed on-demand biometrics, an alternative way to log into an online service that replaces textual passwords with fingerprint authentication on a user's mobile phone [19]. Moreover, many companies have decided to join FIDO Alliance [14], which is an industry consortium promoting the transition from passwords to stronger authentication including fingerprint authentication. This is not only because they have the social responsibility to provide more usable security systems, but also because they want to contribute to economic loss prevention due to security incidents (e.g., password leakage and account sharing). I believe that fingerprint authentication will be even more common in various devices and systems. Although the present demonstration of Auth 'n' Scan is on a smartphone, my contributions are conceptually applicable to other form-factors.

2.2 Fingerprint-based Interaction

HCI (Human-Computer Interaction) research has explored several methods to exploit fingerprints to enable novel interfaces. An early example of fingerprint recognition used for interaction techniques was a fingerprint user interface demonstrated by Sugiura et al. [44]. A contact to their device executed a command uniquely assigned to each finger. Their system utilized a fingerprint authentication mechanism to distinguish user's fingers. RidgePad used fingerprint recognition to improve touch accuracy by identifying a user and estimating her finger posture [17]. Based on the information, it can estimate the user perceived input point which is a little displaced from the actual contact location. In this manner, RidgePad obtained 1.8 times higher accuracy than the conventional touch input. Fiberio is a tabletop touchscreen system that authenticates users during touch interaction with their fingerprints [18]. They used a fiber optic plate which offers both specular reflection and diffuse transmission in order to capture fingerprints and display images simultaneously. This system enables a wide range of tabletop interactions with user identification or authentication.

Prior research has also utilized the specific characteristics of an RF-based fingerprint sensor for novel applications. Hessar et al. presented an on-body transmission method with smartphones that leveraged a drive signal from the metal edge of the fingerprint sensor [16]. They made modifications to be able to control the drive signal to transmit secret information propagating through human body. In this manner, smartphones can establish secure communication channels with peripherals, such as doorknobs (door unlock with fingerprint authentication) and glucose sensors (sending secret information to wearables).

Although my current main scenario is fingerprint authentication on smartphones, integration of a similar concept to dual-purpose biometrics into the systems above could be possible. For instance, a future FUI [44] could sense cardiovascular data every time a user executes a command. My work contributes to demonstrating the feasibility of gathering physiological data through a short-time interaction (i.e., authentication in this project).

2.3 Unobtrusive Cardiovascular Sensing

Prior work has investigated unobtrusive approaches to sense user's cardiovascular data. Kang et al. developed a mobile electrocardiogram (ECG) monitoring system on a smartphone, called Sinabro [24]. They attached multiple electrodes at the front and back of a smartphone. Sinabro measures the user's ECG when she makes contacts with her left and right body parts. Griffiths et al. integrated an ECG-based heart sensing technique to a chair [15]. Health Chair acquires ECG through electrodes attached to the armrests. One major limitation of ECG sensing is that it requires multiple physical contacts with bare skin. Griffiths et al. found that Health Chair was able to extract user's heart rate information for even shorter than 1% of typical office hours (i.e., 8 hours) in their study. Sinabro requires users to hold a device with both hands, and some users may prefer such bimanual possessing [11]. However, one-handed interaction is also common in mobile touch-screen devices [25]. Thus, sensing opportunities can greatly vary depending on their device holding preferences. My Auth 'n' Scan system allows cardiovascular sensing during fingerprint authentication, and can co-exist with Sinabro.

Prior research has examined alternative approaches to cardiovascular sensing. One method is to use reflection of radio frequency waves. Adib et al. developed Vital-Radio, which can monitor breathing and heart rates of multiple people without physical contacts with the sensor [2]. Their system can detect respiration and heartbeat changes from signals reflected on users' bodies. BodyScan is a wearable system that recognizes various user's activities and

status including heart rates [13]. It consists of a wristwatch-like radio transmitter and receiver with a holster. The system uses the intensity of radio signals to infer user's heart rates.

Research has also investigated vision-based approaches to detecting heart rates. Mauka-Mauka used an Webcam attached to a worker's laptop and confirmed the feasibility of unobtrusive heart rate sensing in a workplace environment [43]. Poh et al. developed a Webcam built-in mirror which detects a user's heart rate while she is looking [33]. Wu et al.'s image processing method, called Eulerian Video, can also extract heart rates and possibly other cardiovascular information from images of a person taken by an unmodified camera [47]. Although these vision-based methods are very promising, image capturing can be inappropriate or even prohibited at public contexts. Thus, non-vision approaches can be more appropriate for mobile cardiovascular sensing.

Researchers have explored the use of inertial sensors for mobile cardiovascular sensing. Aly et al. developed a respiratory rate estimation system, called Zephyr, using accelerometer and gyroscope sensors of a smartphone [4]. When a user places her smartphone onto her chest, Zephyr captures the chest movements caused by breathing. Mohamed et al. expanded this method to enable heart rate estimation [29]. Their system, HeartSense, also captures users' chest movements using an off-the-shelf smartphone, but it only uses gyroscope sensor data based on observations on heart motion mechanisms. These methods are robust and accurate, and do not require any additional hardware equipment. However, measurements with these systems require users to perform explicit interaction (i.e., users have to be still and keep their smartphone on their chests).

PPG is also an optical approach though image capture and processing are not necessary in general. Another advantage of PPG sensors is that their form-factor can be small (e.g., one pair of an LED and photo-detector). Chigira et al. integrated a PPG sensor into a tumbler [8]. It can detect a user's heart rate during beverage consumption. Poh et al. and Holz et al. demonstrated integration of PPG sensors into an earphone [32] and glasses [20], respectively. These devices enable continuous cardiovascular sensing while users are wearing them. These projects demonstrated a potential of PPG sensors. But PPG sensors are susceptible to ambient light, and use scenarios in the projects above are limited to dark conditions. For example, a user's hand holding the tumbler blocks PPG sensors from ambient light [8]. Effect by ambient light is negligible inside an ear canal [32]. A PPG sensor is a promising approach, but its use under a normal light condition is challenging.

2.4 Summary

I discussed the literature about fingerprint-related technology and interfaces as well as unobtrusive cardiovascular sensing. Although much research on these areas exists, one of my contributions is to exploit fingerprint authentication for phone unlock to perform cardiovascular sensing through PPG. My work is similar to Chigira et al.'s project in terms of exploiting user's frequent activities as a sensing opportunity.

As I already discussed in the previous section, my dual-purpose biometrics concept can address two of the major challenges in unobtrusive sensing. This work contributes to broadening the field of unobtrusive sensing and applications of biometric technologies.

Exploiting phone unlock for data collection has also been investigated. Truong et al. demonstrated an interface to replace an unlock slider with swipe gestures for completing microtasks [45]. This interface design allows smartphone users to participate in lightweight data collection about themselves and their contexts. Vaish et al. explored a similar concept for microtask crowdsourcing [46]. Similar to these projects, Auth 'n' Scan exploits phone unlock for physiological sensing, which would benefit a variety of healthcare applications.

Chapter 3

Photoplethysmography (PPG)

I use photoplethysmography (PPG) in the current Auth 'n' Scan prototype. PPG requires physical contacts, but it can be acquired from a single sensing location unlike ECG. Furthermore, its hardware can be simple and easily downsized. These characteristics are desirable in my main use scenario (i.e., phone unlock with fingerprints), and I decided to use PPG in this work though other technologies can be considered in future work. In this section, I explain its principle and physiological information derived from PPG signals.

3.1 Sensing Principle

PPG is an opto-electrical and non-invasive measurement technique that can detect blood volume changes in the microvascular bed of tissue [3]. A simple construction of a PPG sensor comprises an LED and photo-detector. A periphery of the body, such as a fingertip or earlobe, is a commonly-used contact point for PPG. Light from the LED is partially reflected on the skin, and captured by the photo-detector. When blood volume changes occur, the amount of light absorption varies. The photo-detector then detects this variability as an electrical signal.

One of the most common medical applications of PPG is pulse oximetry which can monitor oxygen saturation as well as heart rates in a non-invasive manner. Oxyhemoglobin and deoxyhemoglobin exhibit different absorption performance of red and infrared light. A pulse oximeter utilizes this phenomenon to determine the proportion of hemoglobin bound to oxygen [7]. I used CMS-50E, an FDA-approved fingertip pulse oximeter, to obtain ground truth PPG signals.

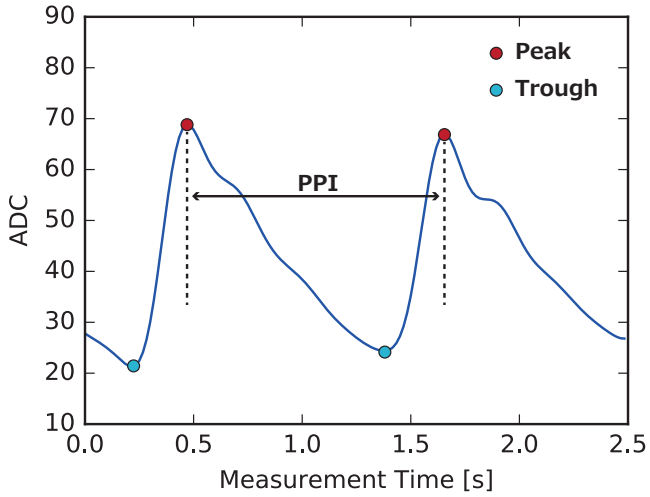

Fig. 3.1 An example of a photoplethysmography signal with CMS-50E. The output can take a discretized value between 0 and 127. Peaks, troughs, and a PPI are annotated.

Figure 3.1 shows a typical waveform gained through CMS-50E with an adult who does not have any major cardiovascular disease. As shown in this figure, a PPG waveform in general demonstrates periodical repetitions. Features in the PPG waveform are denoted as follows:

Peak A local maximum in one cycle.

Trough A local minimum in one cycle.

Peak-to-peak interval (PPI) A time interval between two adjacent peaks.

3.2 Physiological Information Derived from PPG Signals

From raw PPG signals, I can obtain the following physiological information beneficial for personal healthcare applications.

Heart Rate It is derived from the number of peaks per minute. It is one of the most frequently-used cardiovascular features.

Heart rate variability (HRV) It is calculated as the variance of PPIs. It is regarded as a useful feature for assessing an autonomic nervous system.

Poincaré plot It is a plot of two adjacent PPI values. The distribution can be indicative of heart dysfunction [23].

Acceleration plethysmogram It is the second derivative of PPG signals. It can indicate distensibility of the peripheral artery.

Respiration rate It is derived from the frequency of an envelope wave of PPG signals. It is another common cardiovascular feature. Figure 3.2 illustrates how the user's respiratory rate can be derived from a PPG signal.

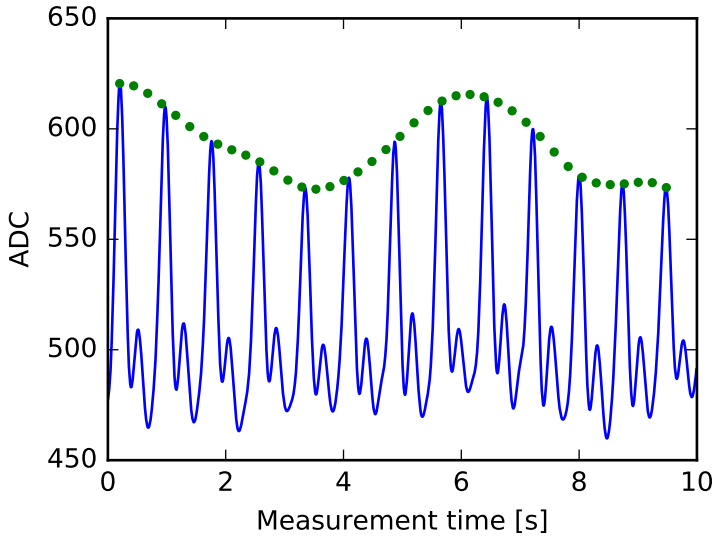

Fig. 3.2 A respiration rate can be derived from the frequency of the envelope of a PPG signal.

Heart rate variability (HRV) is traditionally derived from ECG, but medical research shows that HRV is reliably estimated from PPG [41]. HRV is a well-used feature for assessment of autonomic nervous system dysfunction, but this information can lead to additional observations on cardiovascular activities through a Poincaré plot. In this plot, each point represents two adjacent PPI values. Figure 3.3 illustrates an example Poincaré plot generated from a five-minute long PPG signal with a healthy adult user. A Poincaré plot with healthy users normally demonstrates a distribution that can be approximated as 2D Gaussian [23]. But patients with heart dysfunction can exhibit skewed or dispersed distributions. In general, the creation of a Poincaré plot requires sufficiently-long sampling of PPI, generally for five minutes. Such long sampling is unfortunately impossible in my target application because users would place their fingers for phone unlock only for a couple of seconds. This work examines feasibility to reconstruct a Poincaré plot from a set of short PPG signals.

In a Poincaré plot, $SD1/SD2$ is considered to be one of the most important features. $SD1$ is the standard deviation of the differences of two adjacent PPIs. $SD2$ is the root of the subtract of

$(SD1)^2$ from the variance of PPIs. $SD1/SD2$ is a ratio of these two values. Medical research shows that this metric varies for people with heart or cardiovascular disease [1], and I examine the feasibility of Auth 'n' Scan to extract this feature.

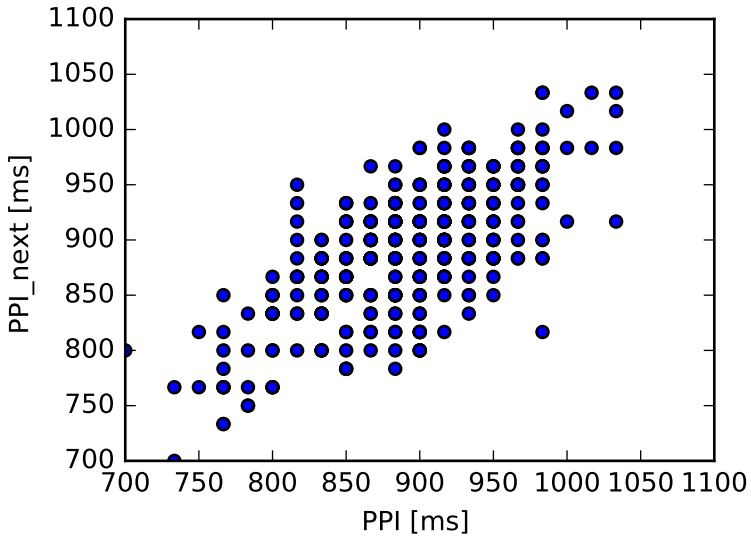

Fig. 3.3 A Poincaré plot generated from PPI data. The shape of the plot can be indicative of a person's heart functionality.

Chapter 4

Implementation

4.1 Sensor Hardware

To instantiate the concept of dual-purpose biometrics in mobile fingerprint authentication, I developed a custom PPG sensor circuit. My circuit is designed to place LEDs and photo-detectors around the fingerprint sensor in a commercially available smartphone. I had the four design considerations in my hardware.

DC-A. *Co-existence with a fingerprint sensor*:
My system performs physiological sensing during fingerprint authentication. As the main application still lies in authentication, my hardware should not degrade or compromise its performance and accuracy. Existing PPG sensors are designed for users to place fingers at the center, but this would not be feasible in my use case. Thus, my hardware should sense PPG from the side of a user's finger.

DC-B. *Sensing under a normal light condition*:
Many PPG sensors function well under sufficiently dark conditions created by finger occlusion or with covers. However, achieving such a dark condition is difficult in typical mobile fingerprint authentication scenarios. My sensors, thus, have to function even under a normal light condition.

DC-C. *Noise and individual difference robustness*:
Users may put their fingers on a fingerprint sensor differently. For instance, users may use a thumb because it allows one-handed interaction, but others may prefer using an index finger. Such a variation can occur even within the same user (e.g., a person may

switch to another thumb for unlock). Even if people use the same finger, placement may be different in each authentication trial. My hardware thus should be able to acquire PPG signals regardless of the user's finger placement.

DC-D. *Instant sensing activation upon touch*:
Because authentication with fingerprint takes only a couple of seconds, my sensor should acquire PPG signals immediately after users place fingers.

Prior work investigated different PPG sensor hardware designs for accurate signal acquisition [3]. However, no circuit design has achieved consensus among the research community. I decided to utilize the PulseSensorAmped [30] hardware for my sensor design. It is an open source PPG sensor project, and its hardware design achieves reliable signal acquisition even under ambient light noise. This hardware includes a differential amplifier with an op-amp, and a raw signal is normalized at 2.5 V and amplified. However, my preliminary investigation found that PPG signals from PulseSensorAmped were saturated for the first few seconds of sensing. When users place a finger on the sensor, a drastic brightness change occurs, which is the main cause of this signal saturation. This is undesirable because a sensing duration in my use scenario is limited.

To avoid saturation, I added two Zener diodes (AZ23C3V3-7-F, 3.3V) to the feedback loop of the negative input channel of an op-amp. Figure 4.1 shows the circuit schematic of my PPG sensor. With these Zener diodes, the amplification rate of this circuit becomes zero when the output voltage would become beyond the range of 0–5 V otherwise. In this manner, my circuit achieves an appropriate gain even when drastic changes in light intensity occur. In addition, I maintain the robustness that the original PulseSensorAmped has. Figure 4.2 illustrates an example observation of PPG signals obtained through PulseSensorAmped and my sensor. I also added a capacitive sensor to the surface of the sensor. This sensor enables instant activation of the PPG sensors. I measured the activation time with an oscilloscope, which turned out to be approximately 300 µsecs. Thus, my hardware design satisfies the design considerations of DC-B and DC-D.

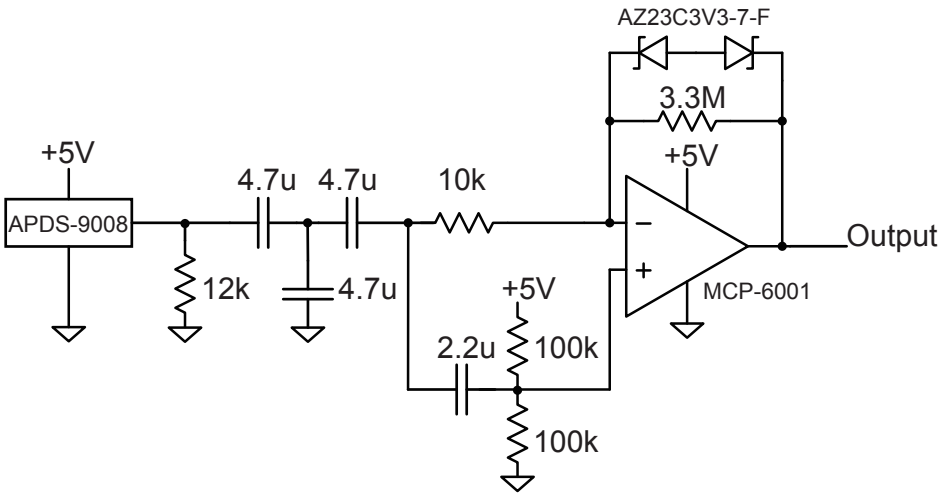

Fig. 4.1 The circuit schematic of my PPG sensor unit. I introduce Zener diodes into negative feedback of an op-amp to avoid signal saturation.

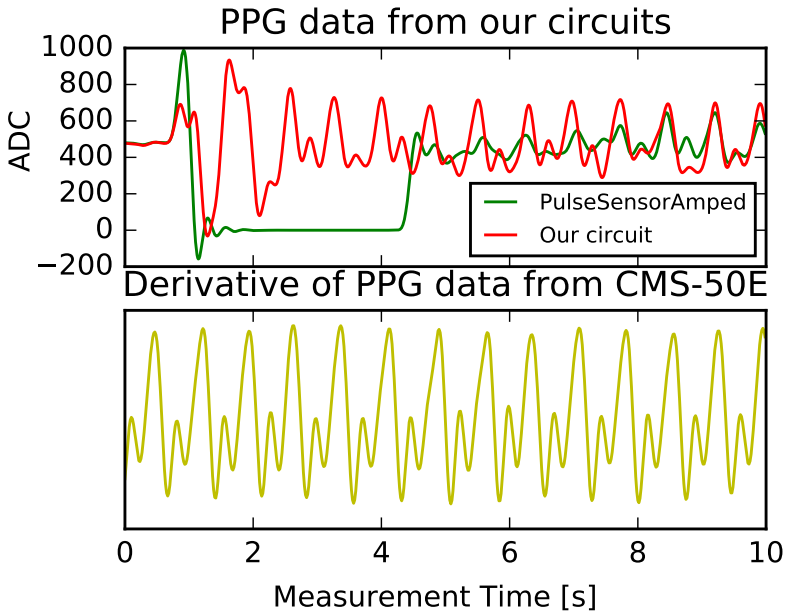

Fig. 4.2 A comparison of an output from my sensor (red), that from the original PulseSensorAmped (green), and the derivative of a PPG signal obtained from CMS-50E (yellow). Note that PulseSensorAmped and a PPG sensing unit in my circuit board return a discretized value between 0 and 1023. The plot of PulseSensorAmped includes negative values caused by a band-pass filter.

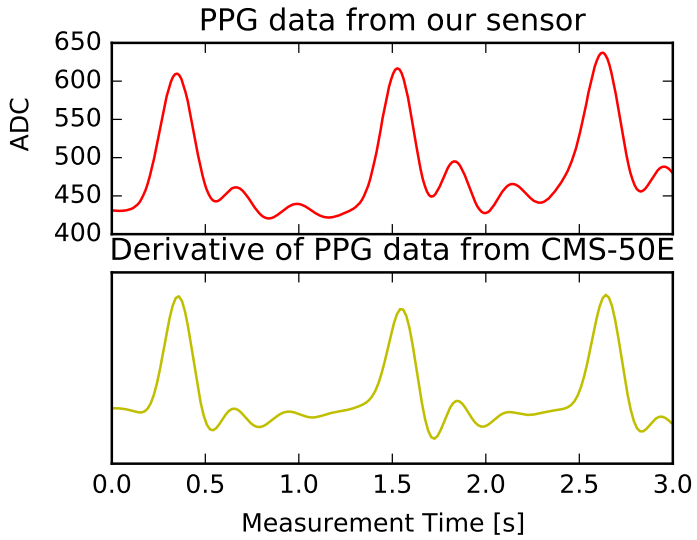

Fig. 4.3 A comparison between an output from my sensor (red) and the derivative of a PPG signal obtained from CMS-50E (yellow). The two signals resemble well.

As my circuit and PulseSensorAmped include differential operations, the appearance of the signal from my sensor is different from a wave shown in Figure 3.1. Figure 4.3 shows a comparison between my sensor output and the first derivative of a signal obtained from CMS-50E. I did not conduct a formal quantitative analysis on the similarity between two signals. However, my preliminary examination confirmed that peaks in at least one of PPG signals correspond well with those in the ground truth. I report accuracy performance of heart rates and HRV from PPG signals in a later section.

Figure 4.4 (C, D) shows the circuit board of my sensor. This circuit board has a space at the top center to fit to the fingerprint sensor on a smartphone (Nexus 5X). The fingerprint sensor on Nexus 5X is attached to the backside of the device. For DC-A and DC-C, I place four PPG sensing units to surround the fingerprint sensor instead of installation at a single particular location. Figure 4.4 (A, B) shows an installation example of my hardware to Nexus 5X. In my current prototype, the sensor is connected to an external computer though more direct integration into a smartphone is possible.

Figure 4.5 illustrates an example of four PPG signals with my sensor. In this example, Channel #4 demonstrates the most similar waveform to the ground truth (the first derivative of CMS-50E signals). A channel which exhibits the most desirable signal is different depending on how users place a finger. My signal processing module automatically selects such a signal as well as extracts features from the raw data, which I explain in the later section.

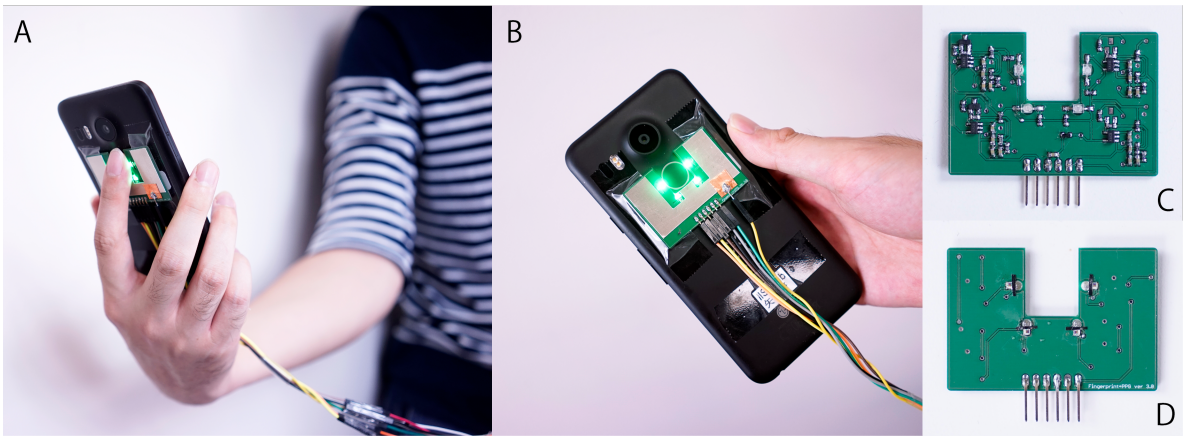

Fig. 4.4 My Auth 'n' Scan prototype hardware. (A) My current prototype is designed for Nexus 5X. (B) The back view of the device. The circuit board places four PPG sensing units around the fingerprint sensor. (C) The back of my circuit. (D) The front of my circuit (without the touch sensor). The LEDs and photo-detectors are designed to be exposed.

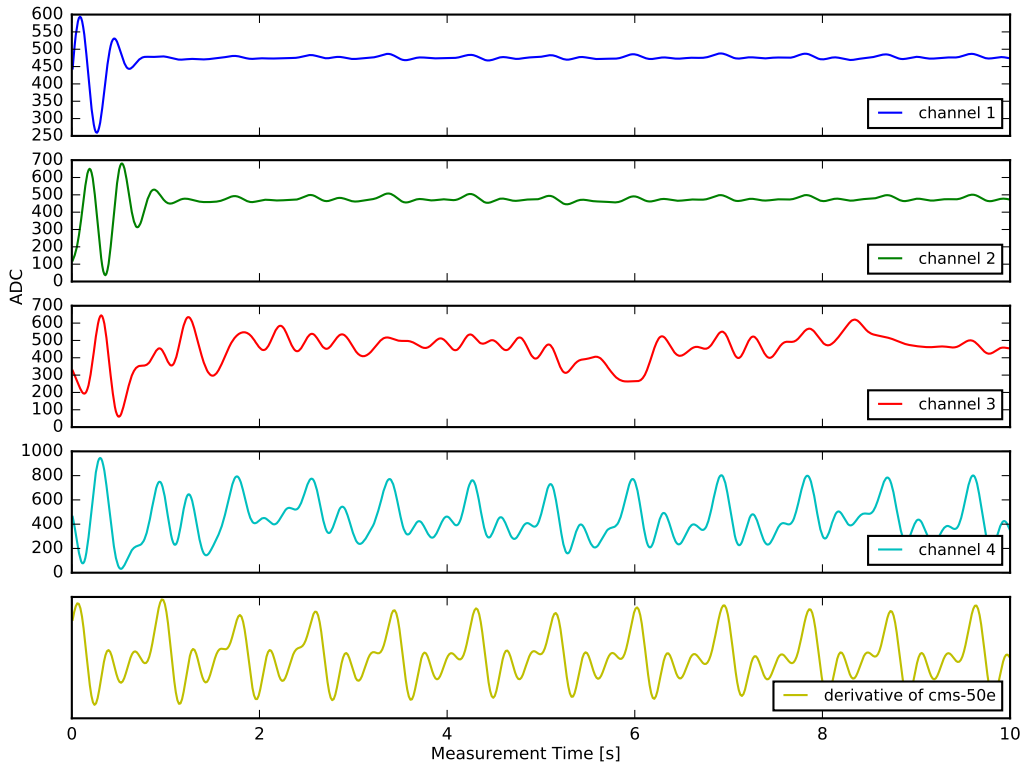

Fig. 4.5 An example of four PPG signals with my sensor and the first derivative of CMS-50E's output. In this example, the Channel #4 (light blue) demonstrates clear peaks that correspond to those in the ground truth signal (yellow) well.

4.2 Informal Hardware Evaluation

I conducted two informal evaluations to validate the robustness of my sensor against ambient noise and finger placement. I used CMS-50E to obtain ground truth data in each experiment.

4.2.1 Ambient light robustness

I recorded PPG signals with my sensor for 10 seconds under the 5 different ambient light conditions. The five conditions included two outdoor and three indoor settings, and the light intensity ranged from 0 to 17280 lux.

Figure 4.6 shows experimental settings and acquired PPG signals. Signals for the first 1500 ms are removed due to large amplitude fluctuation caused by finger contacts as explained in Figure 4.5. My informal test revealed that at least one channel in the sensor demonstrates clear peaks that correspond to the ground truth signal (in yellow) in all conditions. Even under the brightest ambient light condition (the daytime outdoor setting), the peaks in the signal in Channel #2 (in green) match well to the ground truth. I thus concluded that my sensors are robust enough under various ambient light conditions.

4.2.2 Finger placement robustness

I also tested how different finger placement could impact on PPG signals. Similar to the previous informal evaluation, I recorded PPG signals for 10 seconds with 5 different finger directions illustrated in Figure 4.7a. I confirmed that the smartphone could be successfully unlocked by fingerprint authentication at all directions. Measurements were performed under a normal indoor light condition.

Figure 4.7 (b∼f) shows PPG signals acquired under each condition. Again, at least one channel in the sensor shows clear peaks that correspond to the ground truth signal in all conditions. In my current prototype with Nexus 5X, Direction B and D (figure 4.7c and 4.7e) are the most likely finger placement for unlocking with fingerprints. As finger directions vary, the channels which exhibit clear peaks also change (Channel #1 and #2 for Direction B and Channel #3 and #4 for Direction D). This informal study thus validates my sensor design and confirms the robustness against different finger placement.

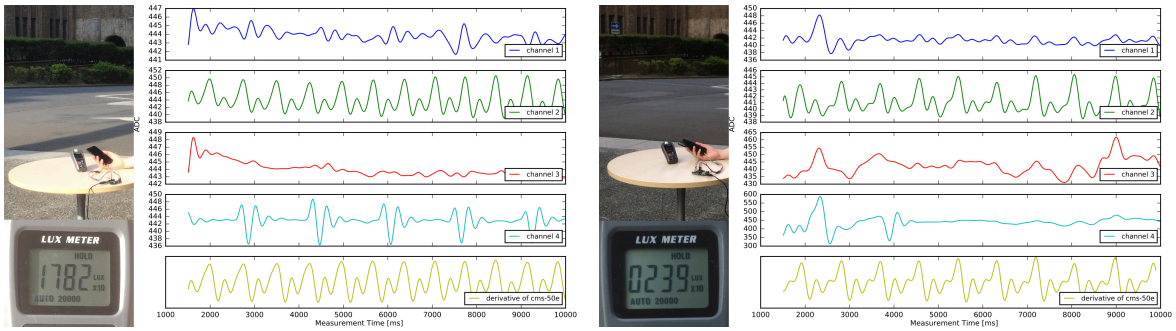

(a) The daytime outside condition (17280 lux).

(b) The evening outside condition (2390 lux).

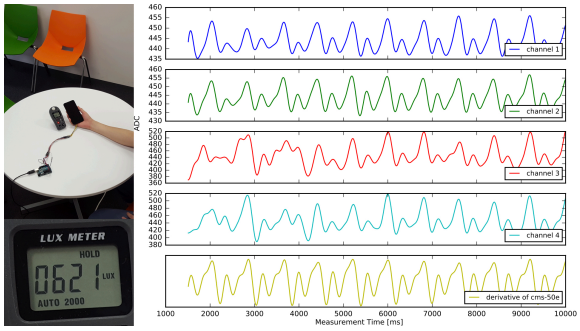

(c) The bright indoor condition (with both sunlight and room light; 621 lux).

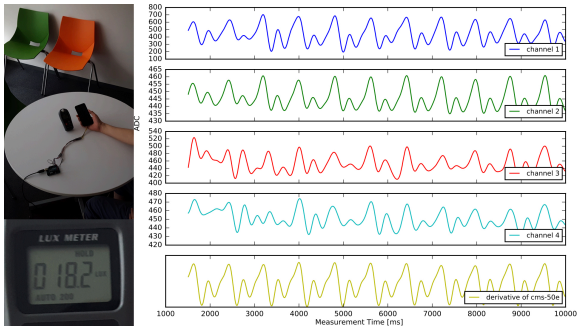

(d) The shadowed indoor condition (with sunlight through a window only; 18 lux).

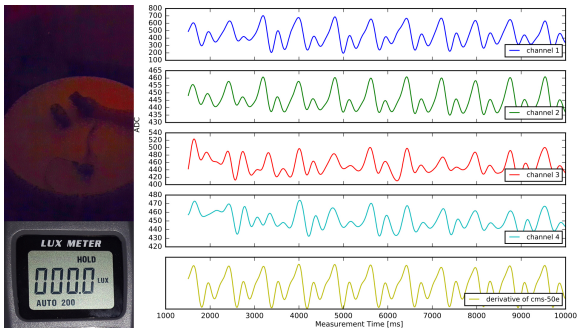

(e) The dark indoor condition (0 lux).

Fig. 4.6 PPG signals under five different ambient light conditions. At least one channel in the sensor demonstrates clear peaks that correspond to the ground truth signal (in yellow) in all conditions.

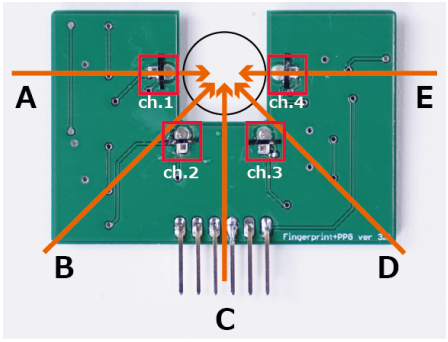

(a) The five finger directions tested.

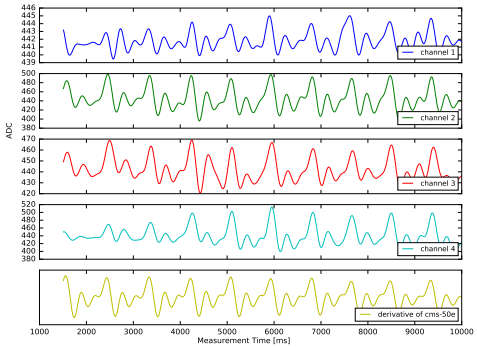

(b) Direction A.

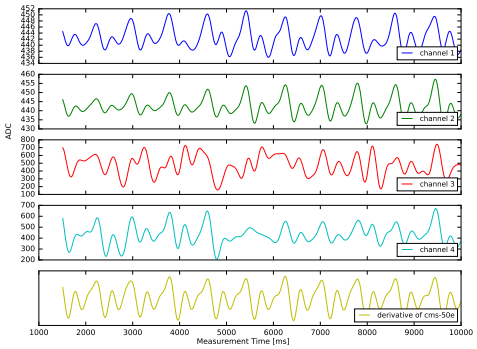

(c) Direction B.

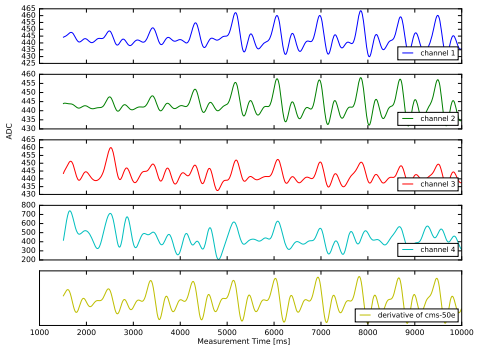

(d) Direction C.

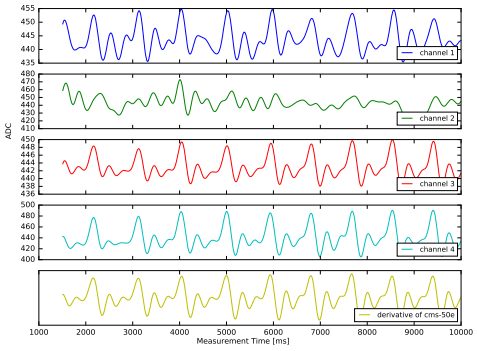

(e) Direction D.

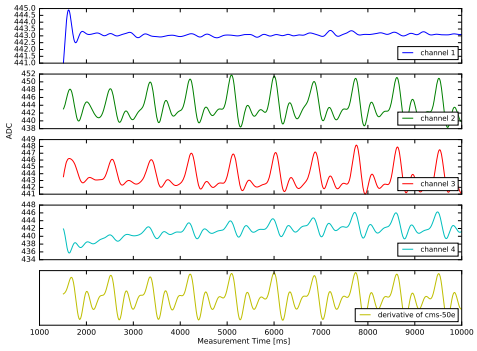

(f) Direction E.

Fig. 4.7 PPG signals under different finger placement conditions. (a): I tested five directions. (b) to (f): Similar to the robustness test against different ambient light, the sensor captured clear peaks at least one channel.

4.3 Frequency-domain Signal Analysis

Although my hardware enables immediate PPG sensing when finger contacts are made, acquired data may have some noise as seen in Figure 4.2. In addition, a sensing duration in my target use scenario is limited to at most a few of seconds unlike conventional PPG systems. I thus need novel PPG signal processing; more specifically, my algorithm has to accurately infer a heart rate and HRV given four few-second PPG signals.

I first conducted a signal analysis using features in the frequency to estimate heart rate from PPG signals [3]. More specifically, I executed the following procedure.

1. Perform a Discrete Fourier Transform (DFT) on each channel of PPG signals with the rectangular window function ($\mathrm{w}(t) = 1$, if $0 \leq t \leq 10$).
2. Detect peaks from the frequency spectra.
3. Select the largest amplitude peak between 0.5 and 3 Hz.
4. Calculate an estimated heart rate as $60 \times$ the frequency of the peak.

Figure 4.8 illustrates an example of the frequency domain spectra for 10-second PPG signals. Plots on the left side show four PPG signals with my sensor and a reference signal with CMS-50E. The graph next to each PPG signal plot displays its frequency spectrum. Inside the right figures, I annotated the estimated heart rate of each signal as well as the reference value acquired from CMS-50E. Although channel #4 demonstrates the most similar waveform to the reference signal, a large difference of roughly 7 beats occur between the reference heart rate (67.3) and estimated heart rate (74.4) obtained in the frequency domain. For comparison, my heart rate estimation method (explained later) estimated 66.7.

The imprecise estimation is due to the frequency resolution in the spectra. The frequency resolution of a DFT is defined as below:

$$\Delta f = \frac{f_s}{N} = \frac{1}{T}$$

where f_s is the sampling frequency, N is the number of data points, and T is the sampling time. From this equation, I can derive the relationship among the sampling time, frequency resolution, and heart rate resolution, summarized in Table 4.1.

This table means that precise estimation would become difficult with shorter sampling time. Therefore, I conclude that frequency domain analysis is unsuitable for my purpose as my system would need to estimate accurate heart rate in shorter seconds.

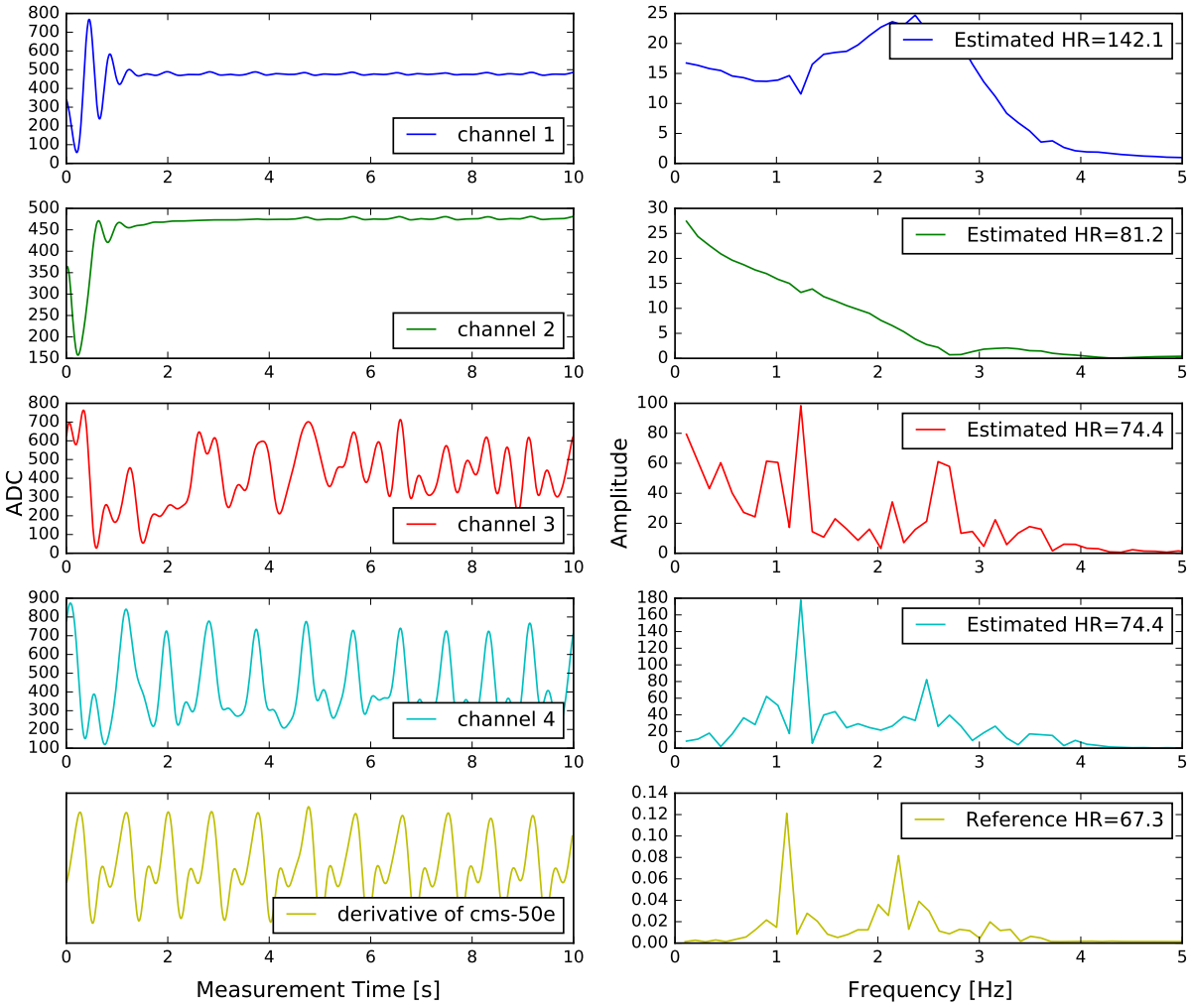

Fig. 4.8 An example of PPG signals and frequency spectra. Left figures show four PPG signals with my sensor and a reference signal with CMS-50E. Right figures show the corresponding frequency domain signals.

Table 4.1 Relationship among the sampling time, frequency resolution, and heart rate resolution.

Sampling time (T) [sec]	Frequency resolution (Δf) [Hz]	Heart rate resolution [beats]
10	0.1	6
5	0.2	12
3	0.33	20

4.4 Heart Rate Estimation Algorithm

The previous section revealed that an approach using frequency spectra is challenging. I thus determined to investigate heart rate estimation methods using time-domain characteristics.

To be informed of the algorithm design, I conducted a pilot study with five people. I asked them to record PPG data with my hardware from the index finger of their dominant hands. After close examinations on the collected data, I obtained two major findings: 1) at least one of the four channels provided clear peaks and good correspondence with the ground truth; 2) such a channel was consistent during sensing. In this example of Figure 4.5, Channel #4 exhibits the clearest signal, but the other channels show noisy signals. The channel which offers the clearest signal varies depending on how users place fingers. But my hardware captures seemingly reliable signals at least one of the channels in most cases. In addition, the most desirable channel does not change within one sensing trial. This is because users do not move fingers or hands; otherwise, authentication may fail. Thus, my algorithm needs to choose the most desirable channel which leads to accurate inference of heart rates and HRV.

To the end, it executes two kinds of processing within and across the channels: 1) finding the earliest point from when PPG gives most plausible results of heart rates and PPIs within each channel; and 2) choosing a channel that shows most peak points and plausible PPI data. In the following explanation, I suppose that the system has obtained four PPG signals for the duration of T seconds. I also denote the signal data of Channel #i between time of t_1 and t_2 as $D_i[t_1, t_2] (i = 1, 2, 3, 4)$.

The algorithm first determines the earliest point (τ^i) from which PPG signals provides plausible heart rates and PPI information in Channel #i. My algorithm applies a bandpass filter between 0.5 and 3 Hz to a raw signal in each channel. This frequency range corresponds to a heart rate between 30 and 180 per minute. The algorithm assumes that major noise caused by initial finger placement occurs at most within the first half (between 0 and $T/2$ seconds) of the entire signals. With this assumption, it extracts $D_i[t, T]$ by varying t from 0 to $T/2$ by 200 ms (i.e., $t \in \{0, 200, 400, ..., T/2\}$).

For each $D_i[t, T]$, it then performs peak detection with the Automatic Peak Detection in Noisy Periodic and Quasi-Periodic Signals method [40]. The algorithm calculates the number of the detected peaks ($P^i(t)$) as well as the mean and standard deviation of the observed PPIs. I then derive a relative standard deviation of the observed PPIs, defined as a ratio of the standard deviation over the mean, denoted as $CV^i_{ppi}(t)$. I also calculate the relative standard deviation of all the peak height values in $D_i[t, T]$, denoted as $CV^i_{ph}(t)$.

After statistics for all $D_i[t, T]$ are calculated, the algorithm next searches τ^i using $P^i(t)$, $CV^i_{ppi}(t)$ and $CV^i_{ph}(t)$ for each t. The algorithm calculates the mean and standard deviation from all values of $CV^i_{ppi}(t)$. It then removes all t such that $CV^i_{ppi}(t)$ is beyond one standard deviation from the mean. As this filtering adaptively changes its threshold, I expect that the system could accommodate data obtained from patients with heart or cardiovascular disease. Similarly, the algorithm removes all t such that $CV^i_{ph}(t)$ is beyond one standard deviation from the mean. A large spike is often observed at the time when a user has made a contact on the fingerprint sensor. This filtering aims to remove signals which contain such drastic fluctuations.

In the remaining set of t, the algorithm further selects t with which $D_i[t, T]$ contained the largest number of peaks. The largest value among such a set of t is chosen as τ^i. This is intended to avoid fluctuations that occurred near the beginning of sensing (caused by a finger contact). After choosing τ^i for each channel, the algorithm selects a channel which exhibits the lowest value of $CV^i_{ppi}(\tau^i) \times CV^i_{ph}(\tau^i)/P^i_{\tau^i}$ (i.e., a channel which contains many peaks, and stable PPI and peak height).

Chapter 5

System and User Evaluation

To quantitatively evaluate the performance of Auth 'n' Scan, I conducted cardiovascular data collection with 10 participants. The following experimental protocol was approved by Research Ethics Committee in School of Engineering, The University of Tokyo (Approval number: KE17-21).

5.1 Data Collection Procedure

At the beginning of the data collection, participants were asked to visit our laboratory at the day when they were available throughout the daytime. After they signed a consent form, I explained the protocol and apparatus to be used. I instructed the participants to see the experimenter every one hour (except the lunch time), eight times in total. For instance, if data collection started at 9 am, the eight sessions occurred at 9:00, 10:00, 11:00, 13:00, 14:00, 15:00, 16:00, and 17:00. All participants started the first session at least at 10:30 so that I collected data during the daytime. HRV is known to have some variability throughout the day [48]. Therefore, this session design is important for me to acquire PPG data at different time of the day.

In each session, participants were asked to perform up to two of the following data collection tasks. During data collection tasks, the participants were seated. Table 5.1 illustrates the design of the eight sessions.

Table 5.1 Tasks in each data collection session.

Data collection	Tasks
Session #1	ShortNormal × 6 times LongNormal × 1 time
Session #2	ShortNormal × 6 times
Session #3	ShortHigh × 6 times
Session #4	ShortNormal × 6 times
Session #5	ShortNormal × 6 times
Session #6	ShortHigh × 6 times
Session #7	ShortNormal × 6 times
Session #8	ShortNormal × 6 times LongNormal × 1 time

ShortNormal Participants unlocked a smartphone equipped with Auth 'n' Scan with their dominant hand, and kept holding fingers for 10 seconds. They also wore CMS-50E on another finger on the non-dominant hand. This data was used for evaluating sensing durations for accurate cardiovascular data inference and reconstructing Poincaré plots. I also recorded if unlock was successful in each trial.

LongNormal Participants attached CMS-50E to a finger on their dominant hand, and recorded PPG for five minutes. This data was used to create ground truth Poincaré plots.

ShortHigh This is the same task as ShortNormal except that participants engaged in lightweight physical exercise (e.g., climbing up and down stairs) before data collection. This simulated a situation in which users have higher heart rates than normal.

I stored all sensor data for later analysis. Before starting the first session, the experimenter registered the fingerprint of each participant's index finger. All sessions were conducted in an office under a normal indoor light condition.

After completing the last session, they were invited to provide subjective impressions about the Auth 'n' Scan system. I first let the participants experience the Auth 'n' Scan system with sensing duration of five and ten seconds. I then conducted a short semi-structured interview to deepen understanding of their Likert scale question responses. None of my participants was native in English. I thus conducted interviews in Japanese and translated quotes to English as faithfully as possible for the report in this thesis.

5.2 Participants

I recruited 10 participants (8 male, Pm1–Pm8; 2 female, Pf1 and Pf2; 22.9 years old on average; 7 right-handed) from my institute for my data collection. Table 5.2 shows the average heart rate for each participant at the beginning of ShortNormal and ShortHigh tasks. None of them claimed to have any known cardiovascular disease, and regularly engaged in intense physical training. All participants were offered approximately 25 USD in a local currency at the end of the data collection.

Table 5.2 Average ground truth heart rates at the beginning of ShortNormal and ShortHigh tasks. I used an pulse oximeter (CMS-50E) to obtain these ground truth heart rates.

Participant	ShortNormal	ShortHigh
Pf1	69.8	90.6
Pf2	77.4	100.4
Pm1	69.7	67.5
Pm2	65.9	75.1
Pm3	71.0	117.2
Pm4	70.8	120.6
Pm5	66.8	92.0
Pm6	63.0	95.7
Pm7	79.8	99.8
Pm8	66.3	94.6

Chapter 6

Results

6.1 CMS-50E Heart Rate Data Validation

I obtained 360 and 120 PPG signal data samples in total for the ShortNormal and ShortHigh tasks, respectively. I first created cardiovascular features from the ground truth signals. Although CMS-50E provides its estimated heart rates, I found that those data exhibited non-negligible fluctuations particularly at the beginning of measurements. This fluctuation affected later heart rate measurements for a relatively long time. Figure 6.1 shows one example measurement observed in my experiment. CMS-50E seems to record a heart rate value every second. However, a log file produced by its accompanying software does not include timestamps, and I was not able to quantitatively validate how much the sampling rate was and how consistent it was. As shown in Figure 6.1, my informal examination found that 20–40 samples were necessary for stable heart rate measurements (which roughly corresponds to 20–40 seconds). In my ShortNormal and ShortHigh tasks, the sensing duration was up to 10 seconds to make each session as short as possible. However, this means that heart rate values provided by CMS-50E may not be stable or accurate in first several trials. I thus decided to examine the raw PPG signal from CMS-50E and extract the heart rate with my algorithm to create ground truth data.

I conducted a comparison to validate whether my algorithm with CMS-50E PPG signal data offered accurate heart rate estimation. In each trial and participant, I had roughly 80 seconds of a PPG signal data from CMS-50E because she was asked to keep placing a finger of the non-dominant hand during a session. I assumed that the participant's heart rate would not drastically change throughout the session, and thus I used the average of last 20 heart rate

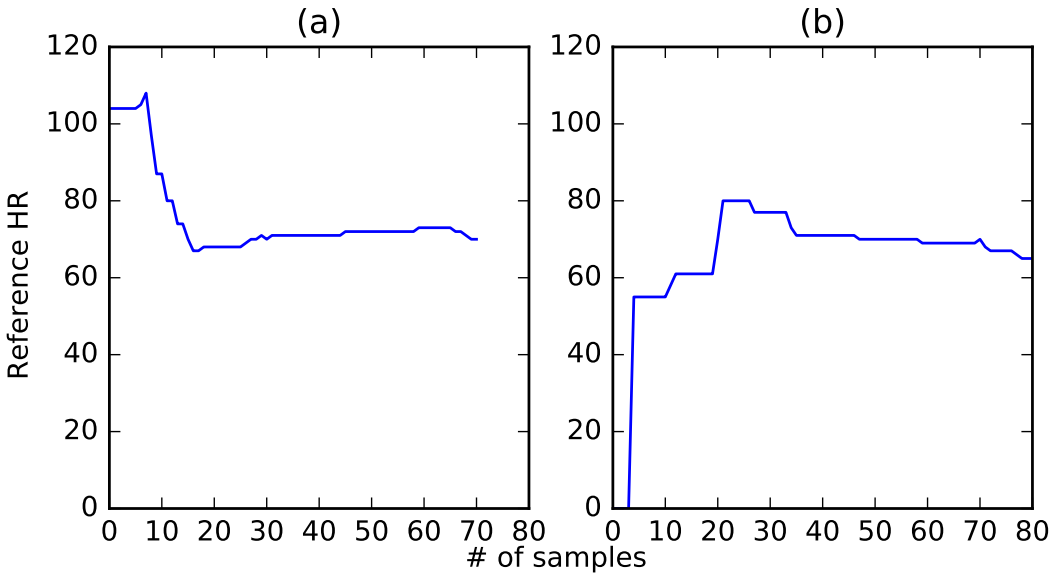

Fig. 6.1 Typical erroneous heart rate measurements in CMS-50E. Note that the sensor seems to record a heart rate approximately every second though no quantitative evidence is available. As shown in these two plots, it can take time to obtain stable heart rate measurements even if a person is sitting at a desk.

samples CMS-50E reports as a reference (HR_r). I then executed my algorithm on PPG signal data from CMS-50E and estimated heart rates (HR_e) for my comparison against the reference values.

Figure 6.2 shows the plot of HR_r and HR_e. I conducted a linear regression analysis, and the result yielded to a line of $HR_r = 0.987 \times HR_e + 2.069$ with $R^2 = 0.92$. As the goodness of fit was high, I concluded that my estimation was sufficient to reliably convert HR_e to HR_r. In subsequent analysis, I calculated HR_r given HR_e extracted from a PPG signal with CMS-50E by using the regression formula above, and regarded it as ground truth heart rate values.

6.2 Heart Rate Estimation

I examined the tradeoff between the sensing duration and accuracy of estimated cardiovascular features. To this end, I created signals with eight different durations (i.e., $T \in \{3, 4, 5, 6, 7, 8, 9, 10\}$) from original data, and execute my algorithm. I removed clear outliers where the ground truth signals were not reliable. The outliers met at least one of the following criteria: 1) the detected heart rate in ground truth data was above 160; 2) the detected heart

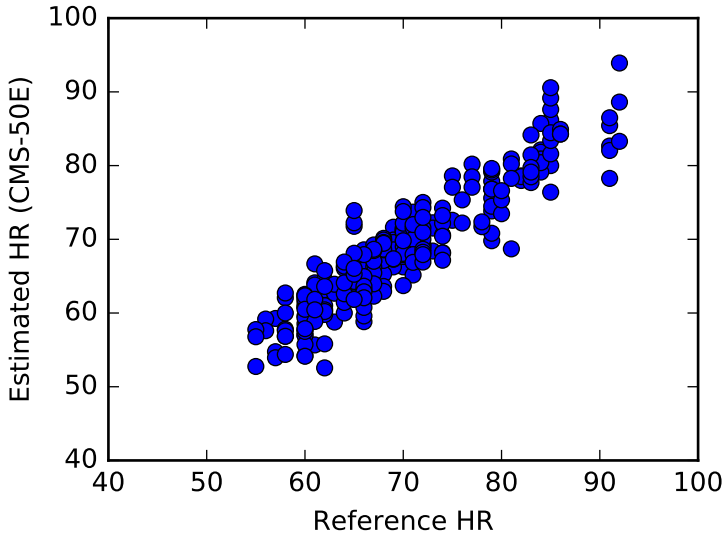

Fig. 6.2 A plot of the reference and estimated heart rate values using CMS-50E. The reference heart rate was the average of the last 20 recording of heart rate values directly produced by CMS-50E. The estimated heart rate is a value my algorithm extracted from the raw CMS-50E PPG signal.

rate in ground truth data was 0; and 3) the standard deviation of PPIs in ground truth data was over 200. As a result, 29 data points (about 6%) were excluded.

I considered five different contexts for heart rate estimation: 1) Both ShortNormal and ShortHigh data (without outliers); 2) ShortNormal data only; 3) ShortHigh data only; and 4) ShortNormal data only with the baseline heart rate information for each participant given; and 5) ShortHigh data only with the baseline. The fourth and fifth conditions are considered as a situation where users would perform baseline measurements similar before starting to use the system. Because fingerprint authentication requires registration before its use, such baseline measurements are plausible. I used the average value of the heart rates detected from the ground truth ShortNormal data for the baseline heart rate estimation. I assumed that heart rates in ShortNormal should be within $\pm$ 20 from this normal-condition value (e.g., if a participant had an average heart rate of 60 under a normal condition, estimation below 40 or above 80 would be discarded). After light exercise, heart rates become faster than in the normal context. I thus performed similar filtering for the fifth condition by ignoring data whose estimation was beyond $\pm$ 20 from the addition of 20 to normal-condition values.

Table 6.1 shows the average differences between the ground truth and estimated heart rates under the five conditions. As expected, a longer duration resulted in higher estimation accuracy. For example, my estimation error can be up to 1.7 even without baseline heart rate information

Table 6.1 The mean differences of the estimated heart rates from the ground truth data. A positive value represents over estimation. The values in parentheses represent the standard deviations.

Duration (T) [sec]	Without the baseline heart rate information		
	ShortNormal and ShortHigh	ShortNormal	ShortHigh
10	1.37 (13.3)	1.69 (13.3)	0.42 (13.1)
9	1.72 (14.1)	2.30 (13.7)	0.03 (15.0)
8	3.66 (18.3)	4.90 (17.2)	-0.03 (20.6)
7	6.50 (22.5)	8.51 (23.0)	0.56 (19.7)
6	11.5 (25.7)	12.5 (25.5)	8.68 (26.0)
5	16.1 (30.5)	17.2 (30.5)	12.9 (30.4)
4	30.2 (34.2)	33.7 (34.4)	19.9 (31.3)
3	40.2 (35.4)	44.8 (35.4)	26.8 (31.6)

Duration (T) [sec]	With the baseline heart rate information	
	ShortNormal	ShortHigh
10	-0.92 (2.93)	1.09 (7.73)
9	-0.69 (3.07)	-0.87 (7.47)
8	-0.39 (3.92)	1.57 (6.59)
7	-0.79 (3.90)	1.45 (7.84)
6	0.01 (5.69)	5.75 (15.6)
5	0.44 (6.89)	5.96 (15.3)
4	1.76 (9.81)	6.40 (16.2)
3	4.14 (7.96)	9.55 (18.1)

under T=10 seconds. However, the standard deviations were relatively large even under the conditions of T=10. As T got shorter, the estimation became further less precise. This result indicates that heart rate estimation without baseline information is challenging.

On the other hand, my estimation was accurate with baseline heart rate information. Even in the case of T=5 seconds, the average difference from the ground truth data was under 1 although the standard deviation was 6.9. In a shorter sensing duration, the average difference did not change greatly but the standard deviation became much larger. The results in the sensing duration of three seconds seemingly showed decent performance. However, I note that many data samples were filtered out in this case. Therefore, I concluded that the best T in my experiment was five seconds.

Figure 6.3 and 6.4 show a visual comparison of scatter plots between the ground truth and estimated heart rates for three durations (3, 5, and 10 seconds) with and without baseline heart rate information. This comparison clearly illustrates the positive effect of the baseline heart rate information. As shown in Figure 6.4, filtering successfully maintained many data

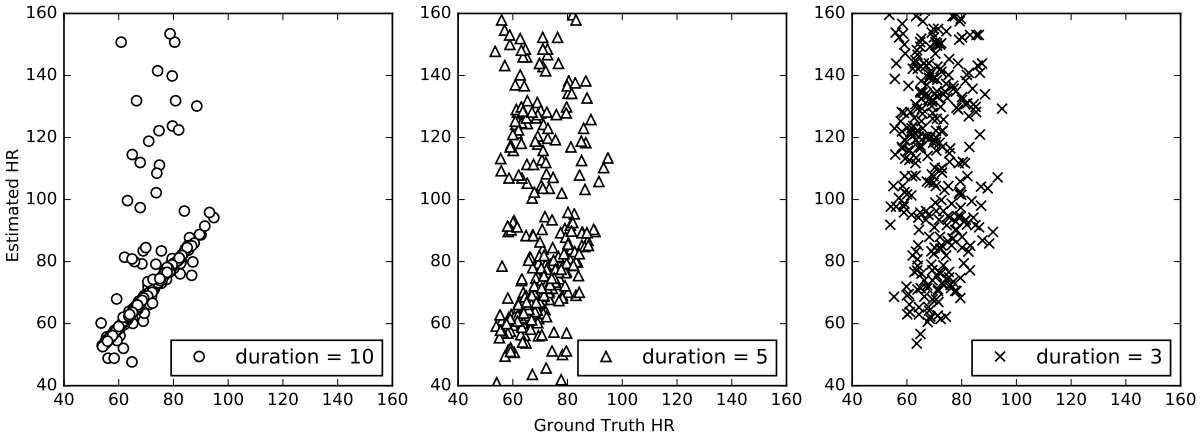

Fig. 6.3 A scatter plot of heart rate estimation from ShortNormal data without the baseline heart rate information. As the sensing duration becomes shorter, more of erroneous data samples are observed.

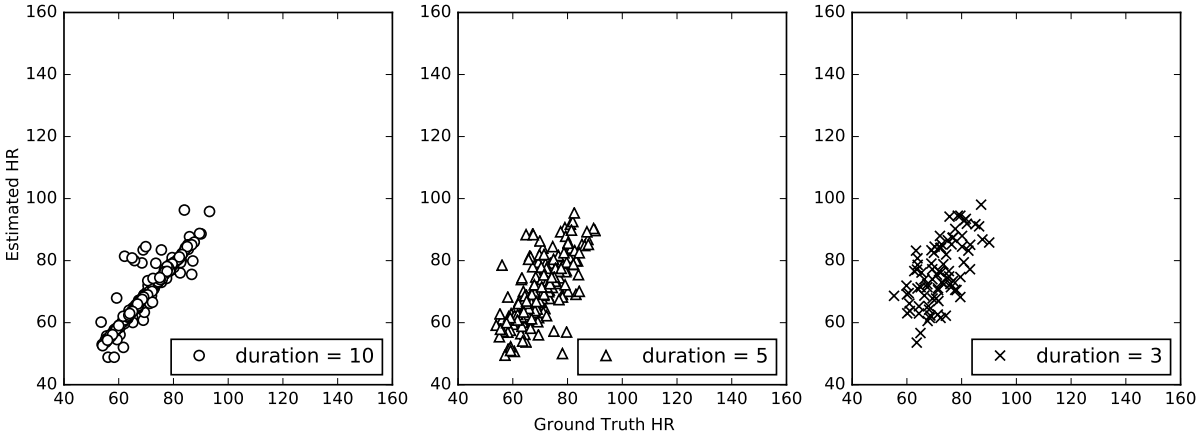

Fig. 6.4 A scatter plot of heart rate estimation from ShortNormal data with the baseline heart rate information. Compared to Figure 6.3, erroneous data samples are successfully removed.

samples that are highly correlated with the ground truth data. This successful filtering resulted in greatly improved accuracy and precision on heart rate estimation.

My results also revealed that accuracy of heart rate estimation was not largely different between ShortNormal and ShortHigh under the absence of baseline heart rate information. However, this result differed if the baseline heart rate information was available. The accuracy was improved in both settings, but the standard deviations were much larger with ShortHigh data than ShortNormal. This suggests that heart rate sensing after light exercise is challenging though this work shows a potential.

6.3 Poincaré Plot Feature Estimation

I examined how accurately I can obtain features in Poincaré plots by reconstructing them from ShortNormal data. I first investigated how many PPIs can be extracted given T. As a PPI requires two peaks, the necessary sensing duration would be longer than for heart rate estimation. Table 6.2 shows the mean number of extracted PPIs across different T. In the heart rate estimation, T=5 was the best; however, this value would result in a limited number of PPI data points. To examine the best estimation performance of Poincaré reconstruction, I decided to set T=10 in this part of my evaluations.

Table 6.2 The mean PPI data points that were able to be extracted in different sensing duration T. The values in parentheses represent the standard deviations. In later analysis on Poincaré reconstruction, I used T=10 as it provided a sufficient number of samples.

Duration (T) [sec]	Mean # of PPI data points
10	135.5 (16.8)
9	100.7 (16.3)
8	70.4 (11.9)
7	45.7 (10.9)
6	26.3 (6.39)
5	11.8 (6.79)
4	1.90 (1.64)
3	0.20 (0.40)

I evaluated differences of $SD1/SD2$ between the ground truth signal and ShortNormal data with T=10. Figure 6.5 and 6.6 illustrate these differences across all participants. As HRV data can vary throughout the day, I compared estimated $SD1/SD2$ from all ShortNormal data for each participant with her LongNormal data gathered in the first and last sessions separately. These plots suggest that estimation of $SD1/SD2$ was fairly accurate for four participants (Pm3, Pm6, Pm7, and Pm8) though not all.

Figure 6.7 shows the Poincaré plots created with the LongNormal and ShortNormal data for Pm6. In his case, the two Poincaré plots produced with the two LongNormal data were similar (the left and center plots in Figure 6.7). As a result, reconstruction from his ShortNormal data also yielded to a small difference in $SD1/SD2$.

Figure 6.8 shows the Poincaré plots created with the LongNormal and ShortNormal data for Pm1. His Poincaré plots produced with the two LongNormal data showed different

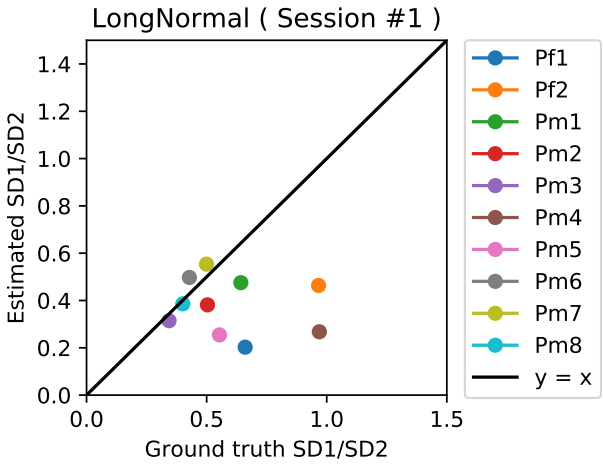

Fig. 6.5 Differences of $SD1/SD2$ in Poincaré plots between all ShortNormal data and LongNormal of the first session.

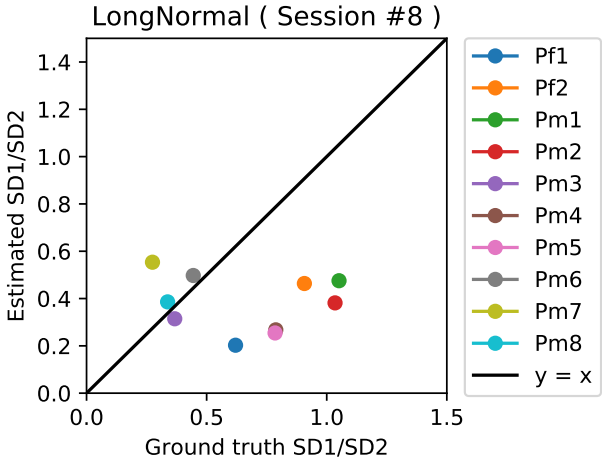

Fig. 6.6 Differences of $SD1/SD2$ in Poincaré plots between all ShortNormal data and LongNormal of the last session.

distributions (the left and center plots in Figure 6.8). The plots moved toward the top right as it became later of the day. This tendency was also observed in the reconstructed Poincaré plot with his ShortNormal data (the right plot in Figure 6.8). This may be one reason for inaccurate estimation of $SD1/SD2$. A future algorithm can be time-sensitive to obtain more accurate reconstruction (e.g., using only data gathered in a particular time period).

In conclusion, although individual differences need to be considered, reconstruction of Poincaré plots from a set of fragmented data can be possible if a sensing duration was long enough (e.g., 10 seconds).

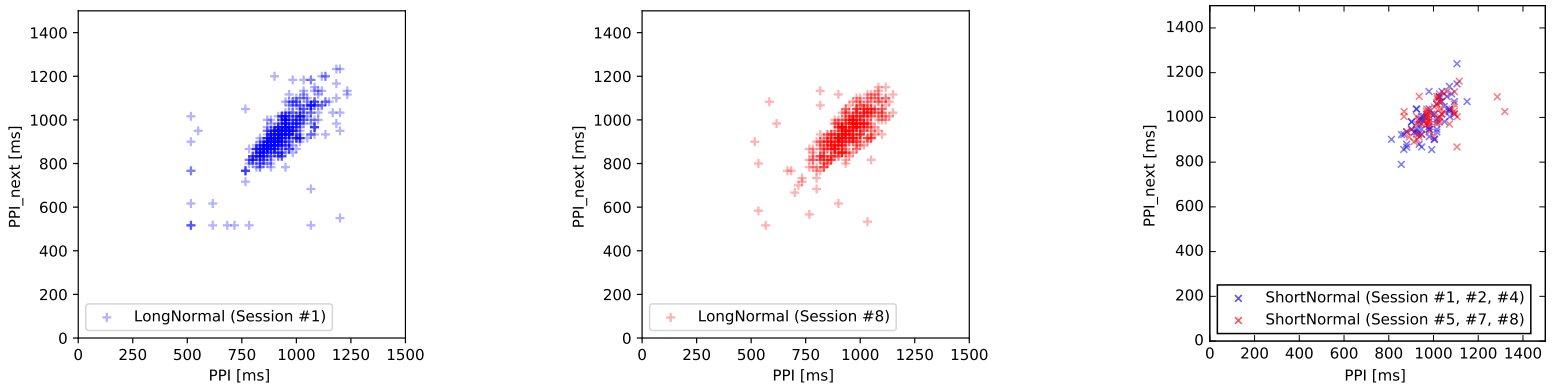

Fig. 6.7 Poincaré plots for Pm6. Left: the Poincaré plot with the LongNormal data in the first session. Center: the Poincaré plot with the LongNormal data in the last session. Right: the Poincaré plot reconstructed with the ShortNormal data (blue: data in Session #1, #2, #4; red: data in Session #5, #7, #8). In the case of Pm6, variability over time was small, and reconstruction of a Poincaré plot was relatively successful.

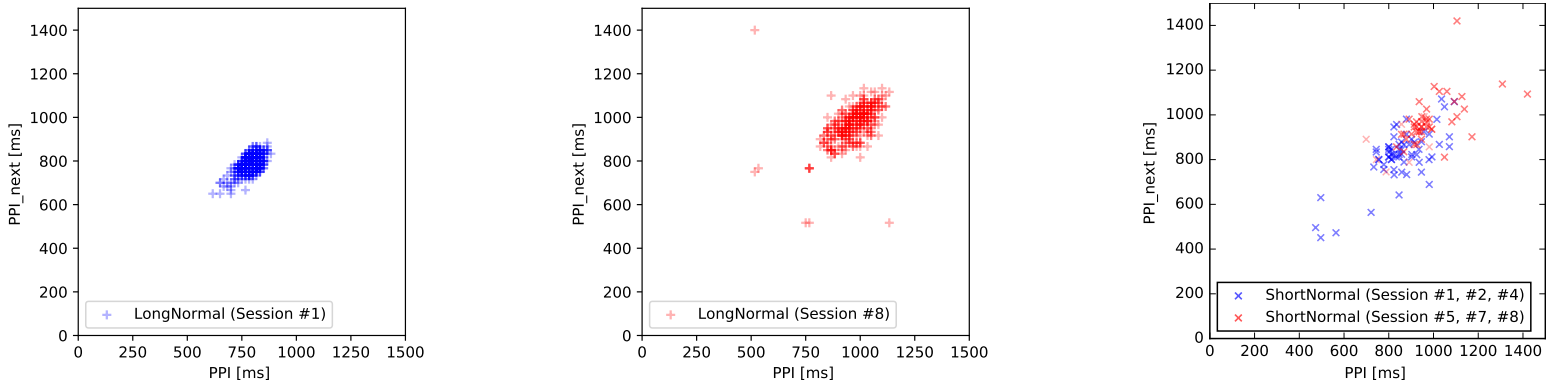

Fig. 6.8 Poincaré plots for Pm1. Left: the Poincaré plot with the LongNormal data in the first session. Center: the Poincaré plot with the LongNormal data in the last session. Right: the Poincaré plot reconstructed with the ShortNormal data (blue: data in Session #1, #2, #4; red: data in Session #5, #7, #8). The left and center plots clearly demonstrate variability over time. This variability was clear in the right figure. Although reconstruction using all ShortNormal data was not very successful, this plot suggests that a time-sensitive algorithm could produce an improved result.

6.4 Acceleration Plethysmogram Feature Estimation

I also examined whether I could acquire acceleration plethysmogram features from the signals of my sensors. Figure 6.9 shows an example of acceleration plethysmogram, which is the second derivative of a PPG signal. An early systolic positive and negative wave are called a-wave and b-wave, respectively. The ratio of amplitudes of b-wave to a-wave (b/a ratio) is positively correlated to the risk of cardiovascular heart disease [12]. I examined how accurately my algorithm can estimate this ratio. I used the average value of the ratios over the selected channel's time segment chosen by my algorithm.

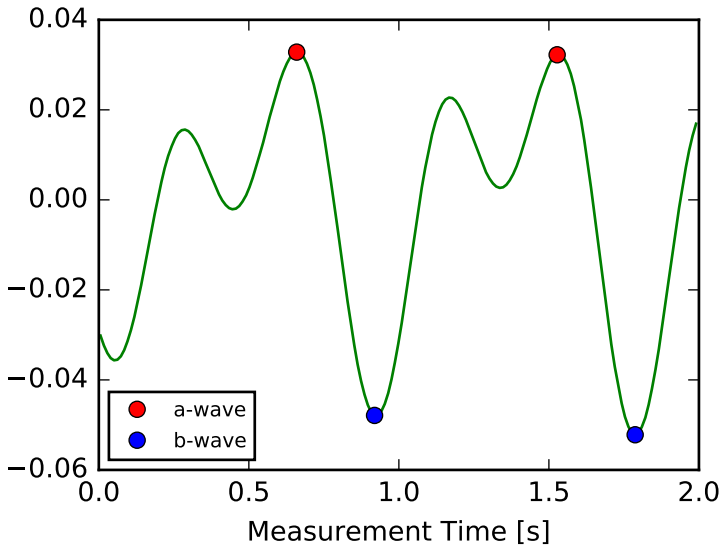

Fig. 6.9 An example of acceleration plethysmogram signals. The signal is the second derivative of PPG signals. A-waves and b-waves are annotated. I used the ratio of heights of b-wave to a-wave as a feature of acceleration plethysmogram signals.

Figure 6.10 illustrates a scatter plot of b/a ratio estimation created from the ShortNormal data with the baseline data (T=10). I conducted a linear regression analysis, and I could not see almost any relationship between the b/a ratio of CMS-50E and Auth 'n' Scan ($R^2 = 0.023$). The plot suggests that the current prototype of Auth 'n' Scan cannot accurately infer b/a ratios. In order to investigate why accurate estimation was difficult, I compared the difference of b/a ratio to the absolute difference of the heart rate (Auth 'n' Scan - CMS-50E). Figure 6.11 shows the scatter plot of the comparison. Even when my system was able to accurately estimate a heart rate, a b/a ratio failed to be inferred. A b/a ratio is vulnerable to even small noise. Such noise in original signals can become non-negligible for estimation of b/a ratios.

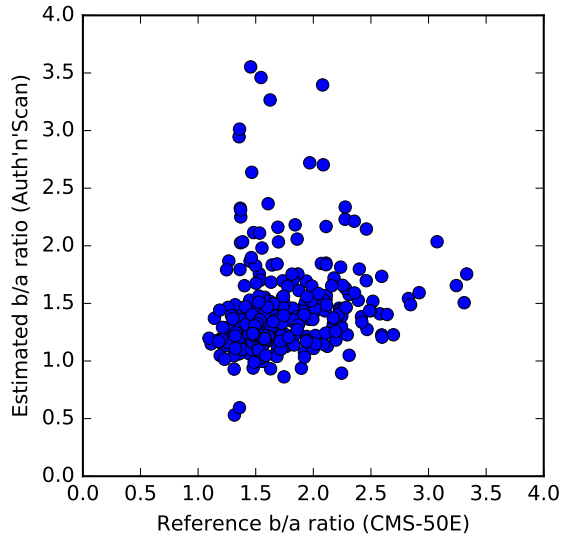

Fig. 6.10 A scatter plot of b/a ratio estimation from ShortNormal with the baseline data. No clear relationship was observed between the reference and estimated b/a ratios.

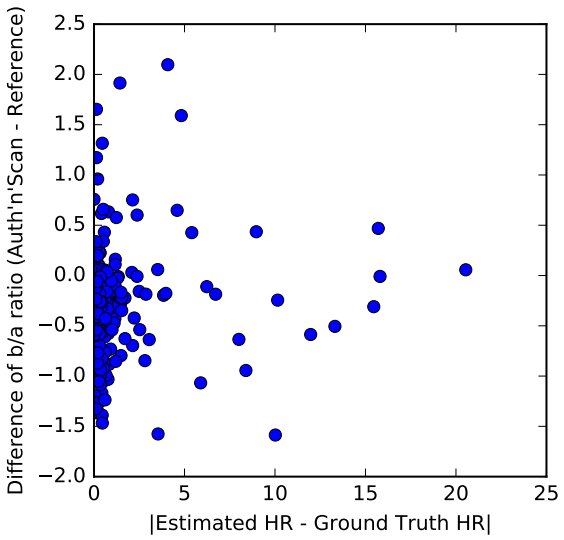

Fig. 6.11 A scatter plot between the difference of a b/a ratio to the error of heart rate estimation. Estimation of b/a ratios was imprecise even for the cases where heart rate inference was precise.

Figure 6.12 shows an example that I was able to perform good b/a ratio estimation from Pm8 data. In this example, the derived acceleration signal (right figure, blue) was clear and similar to the reference acceleration signal (right figure, yellow). The estimated b/a ratio (1.41) was also close to the reference ratio (1.39). However, my result suggests that precise b/a ratio estimation is challenging in the current prototype.

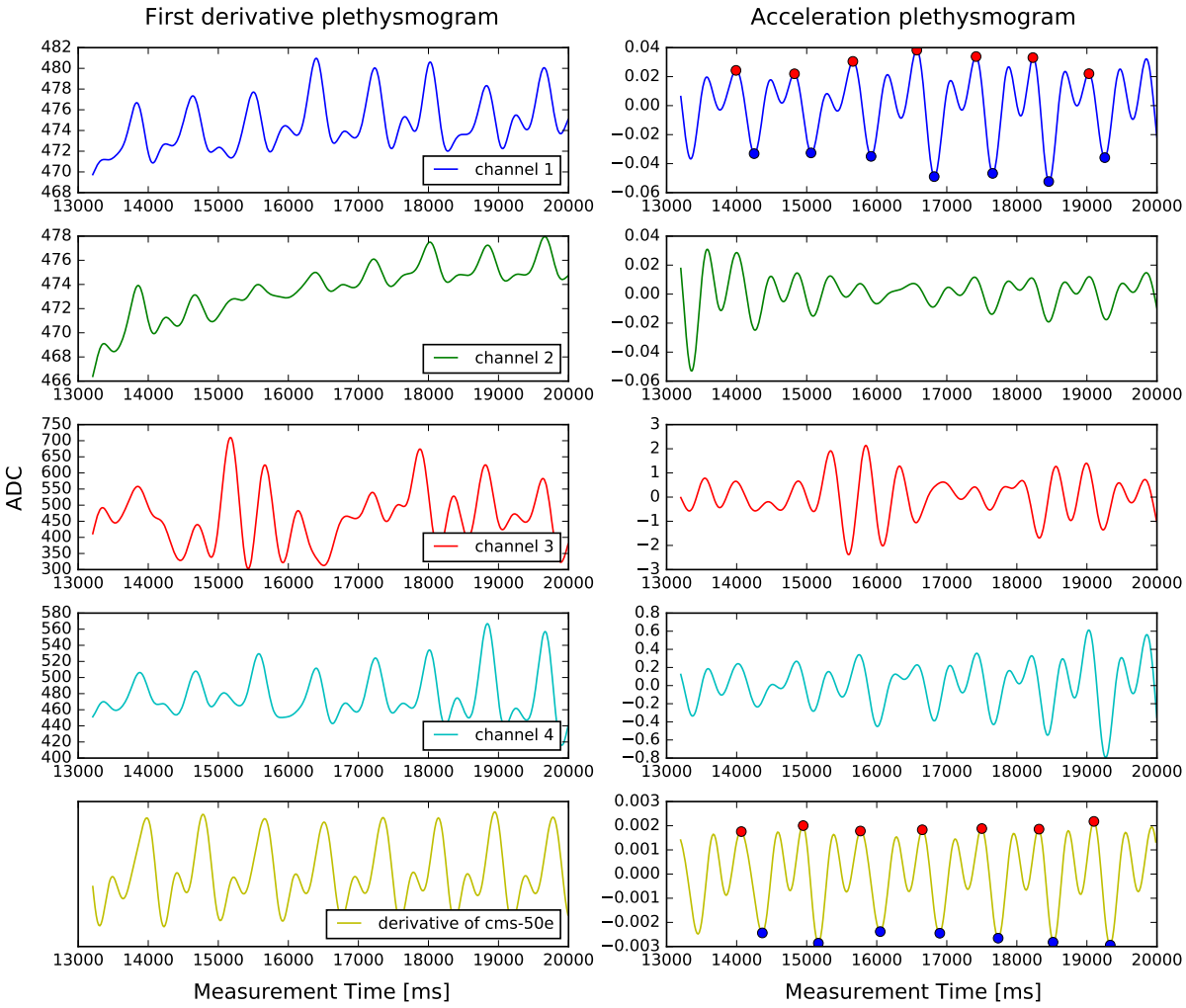

Fig. 6.12 An example of b/a ratio estimation (data from Pm8). Left figures show PPG signals acquired with my sensors and CMS-50E. Right figures show acceleration plethysmograms. In this example, the estimated b/a ratio (1.41) was very close to the reference (1.39).

6.5 Fingerprint Authentication Success Rate

I also examined how the Auth 'n' Scan hardware can impact on the performance of unlocking with fingerprint authentication. All participants were invited to come back for this part of the study in another day. In each trial, the participants were asked to unlock the phone with their fingerprints. Each participant performed 48 trials with and without the Auth 'n' Scan hardware. I defined a trial in which participants were able to unlock a phone as a success. Table 6.3 shows the result of unlock success rates with and without Auth 'n' Scan. The mean unlock success rate with Auth 'n' Scan was the same (96.9%) though the standard deviations

were different (2.46 and 4.20 for with and without Auth 'n' Scan, respectively). I did not observe clear differences in the handedness and gender (right-handed: 96.7% (SD=2.65); left-handed 96.7% (SD=2.41); male: 97.4% (SD=1.85); and female: 94.8% (SD=4.42)). I ran mixed effect linear regression against the following factors: *Condition* (1: with and 0: without Auth 'n' Scan); *Gender* (1: male and 0: female); and *Handedness* (1: right- and 0: left-handed). None of the coefficients for the three factors were significant. The estimated coefficients for *Condition*, *Gender*, and *Handedness* were 0.00 (*SE*: 1.58), -0.73 (*SE*: 2.21), and -0.21 (*SE*: 1.94), respectively. Overall, the accuracies were high in both conditions, and I did not see clear degradation on authentication by introducing Auth 'n' Scan.

Table 6.3 Mean unlock success rate comparison. The values in parentheses represent the standard deviations.

Participants	With Auth 'n' Scan	Without Auth 'n' Scan
All	96.9% (2.46)	96.9% (4.20)
Right-handed	96.7% (2.65)	97.0% (4.79)
Left-handed	97.2% (2.41)	96.5% (3.18)
Male	97.4% (1.85)	96.1% (4.38)
Female	94.8% (4.42)	100% (0)

6.6 Subjective Results

Before the semi-structured interview, I asked each participant to respond to the five 7-point Likert scale questions in Table 6.4.

6.6.1 Acceptability of Auth 'n' Scan

As shown in Table 6.4, my participants expressed their interests in Auth 'n' Scan for everyday use. Comments from my participants were in line with this result.

> *It's not like I want to know health information by wearing wearable devices, but I would want to record it if I can by routine interaction [on a smartphone].* [Pf2]

They also appreciated the unobtrusiveness of sensing by Auth 'n' Scan.

> *I would easily give up if I have to do recording by myself. But a system like this would be easy to use because it automatically collects information.* [Pm1]

Table 6.4 Questions and responses about subjective impressions on Auth 'n' Scan.

Question	Median	Quartile	Mode	Max	Min
As a dual-purpose biometrics system, how much would you like to use Auth 'n' Scan in a real life? (1: do not want to use at all – 7: want to use it every day)	7	6.25 (1st) 7 (3rd)	7	7	5
How acceptable would it be to wait for 5 seconds when you use fingerprint authentication? (1: definitely unacceptable – 7: definitely acceptable)	5.5	4.25 (1st) 6 (3rd)	6	7	3
How acceptable would it be to wait for 10 seconds when you use fingerprint authentication? (1: definitely unacceptable – 7: definitely acceptable)	2	2 (1st) 3.75 (3rd)	2	6	1
How acceptable did you think the interference by my hardware was? (1: definitely unacceptable – 7: definitely acceptable)	5.5	4.25 (1st) 6 (3rd)	6	7	3
How acceptable would it be to monitor your cardiovascular information with Auth 'n' Scan from the perspective of privacy? (1: definitely unacceptable – 7: definitely acceptable)	7	7 (1st) 7 (3rd)	7	7	7

6.6.2 Acceptable sensing duration

My system evaluation found that Auth 'n' Scan would need five seconds for accurate heart rate estimation. The responses from my participants generally showed that this duration was acceptable. My qualitative results also corroborated with this result.

> *I didn't feel (5 seconds) was that long. I don't want to wait when I am in a rush, but I don't mind either because it's just a little long.* [Pm3]

> *Fingerprint authentication does not respond quickly with my finger anyway. So five seconds don't matter to me.* [Pm2]

However, two of the participants (Pm1 and Pm6) expressed that five seconds were slightly unacceptable. Furthermore, when the sensing duration became ten seconds, my participants mostly agreed that it was not acceptable. With this duration, they felt that sensing became rather obtrusive. These results suggest that the sensing duration of five seconds is acceptable though a shorter duration would further improve the acceptability of Auth 'n' Scan.

6.6.3 Perceived interference by hardware

As shown in Table 6.4, my participants did not feel that the sensor board strongly interfered with their fingerprint authentication. This result also positively supports my concept. Three of the participants, though, felt a little discomfort due to the thickness of the hardware (2.3 mm thick in the current prototype). However, as I showed in Section 6.5, the installation of the hardware did not significantly degrade the authentication performance.

6.6.4 Privacy concerns

I obtained unanimous strong agreement from the participants that recording cardiovascular information with the Auth 'n' Scan does not raise privacy concerns. Representative reasons were: heart rate information cannot be directly used for identification (3 participants); heart rate information is not sensitive data (3 participants); and it is acceptable as long as data are securely kept (2 participants). Existing mobile apps can also collect heart rate information and potentially more intimate physiological data. My participants thus did not have strong reluctance for heart rate sensing with Auth 'n' Scan.

Chapter 7

Discussion and Limitation

7.1 Discussion

My results on the heart rate estimation found that inference was accurate when baseline heart rate information is available though its precision needs improvements. In particular, a sensing duration of and above five seconds can lead to accurate heart rate estimation. Such baseline measurements are feasible when users are asked to register their fingerprints before the use of an authentication feature. Because my hardware performs PPG sensing from the side of a finger unlike existing systems, accurate heart rate estimation is challenging. In addition, I conducted my evaluations under a normal light condition. My work, thus, still offers unique contributions for heart rate estimation with a limited sensing duration.

My evaluations also revealed that the sensing duration should be at least five seconds with my current prototype. This is longer than time users would normally spend for unmodified fingerprint authentication. However, subjective responses from my participants confirmed that the sensing duration of five seconds was acceptable. Their quotes suggested that this positive response was mainly because my system does not require separate explicit measurements of heart rates. Future work should investigate how to improve the acceptability of the system besides shortening the sensing duration. A future system, for example, could offer a quick way to opt in and out opportunistic PPG sensing by pressure-sensitive contacts. When users make a contact with pressure, the system would not execute sensing and simply unlock a phone. Otherwise, it would perform PPG sensing for five seconds (and even longer if users are willing) and execute phone unlock. I admit that future work should further investigate how to shorten

the sensing duration. But my work demonstrates sufficient feasibility of opportunistic PPG sensing during fingerprint authentication.

The results confirmed that heart rate estimation becomes unreliable without baseline information. Although the performance degradation was expectable, my results showed its strong effect. In particular, standard deviations of estimated heart rates were large; in most cases without the baseline, they were over ten. Possible factors may have caused this large variance. In some trials, finger placement may not have been close enough and PPG sensing became noisy. I also observed that participants unintentionally performed observable motions, causing large fluctuations in PPG signals (e.g., adjusting their holding of the device). Such motions occurred regardless of the presence of the Auth 'n' Scan hardware, and could have contributed to similar authentication failure rates. Without the baseline heart rate information, my algorithm cannot remove outliers caused by the factors above. This led to large performance degradation.

My results revealed that heart rate estimation often becomes inaccurate after participants took light exercise. One possible reason for this phenomenon is that jittering of the hand and arm holding the device was observable, potentially caused by harder respiration. Smartphones can easily distinguish whether a person has engaged in light exercise with inertial sensors [27]. Thus, a future system can ignore samples after exercise or perform necessary adjustment on estimated heart rates.

I also examined the feasibility of reconstructing Poincaré plots from a set of fragmented PPI values extracted from my sensor data (T=10). The results showed that it can be possible, but future work should examine improvements which handle variability observed over time. As I briefly discussed in the result section, a time-sensitive algorithm may help. A future system could encourage users to unlock a device if enough data samples are necessary for a short period (e.g., deliberately introducing a notification about minor events when users may feel boredom [31]). Future systems should investigate how to exploit user's interruptability for more frequent data collection as well as improve my algorithm in order to obtain reliable estimation results.

My quantitative examinations also confirmed that integration of Auth 'n' Scan did not degrade fingerprint authentication performance. As none of my participants owned the same smartphone used in Auth 'n' Scan (i.e., Nexus 5X), they did not have prior experience with its particular fingerprint sensor. Some participants also commented that they often could not find finger sensor location precisely because it is on the back of the device. In my tasks, participants

were instructed not to re-adjust their finger placement even if they failed to unlock. Thus, my results could be considered as one of the worst performance cases. Nevertheless, the results showed comparable success unlock rates regardless of the presence of the Auth 'n' Scan sensor. I concluded that Auth 'n' Scan did not greatly diminish authentication accuracy upon phone unlock in my experiment.

Subjective responses from my participants also confirmed positive aspects of the current Auth 'n' Scan prototype. Despite the bulkiness of the prototype, the participants did not feel strong discomfort. As future systems may employ thinner hardware or more direct integration into a smartphone, physical interference caused by the hardware could be minimized. The participants unanimously agreed that collecting cardiovascular information through Auth 'n' Scan would not create strong privacy concerns. This is an encouraging result for Auth 'n' Scan and a larger set of dual-purpose biometrics systems. Although additional user studies would be necessary to investigate social acceptability and privacy concerns in a realistic setting, this work demonstrates a potential of the viability of Auth 'n' Scan.

7.2 Limitation

My results suggest that opportunistic PPG sensing during fingerprint authentication on a smartphone is feasible. I now discuss several limitations of this work for clarifying its contributions and possible future research.

I employed a naïve heuristics with baseline heart rate information to remove noisy data. Using built-in sensors, smartphones can sense activities which lead to different levels of heart rates (e.g., sitting, walking, and running). However, users may exhibit different frequencies of carrying smartphones [10, 28]. Thus, an assumption that Auth 'n' Scan can adjust heart rate inference using built-in sensors may not hold for some users. Future work should investigate other methods for intelligently calibrating baseline heart rates.

I examined the performance of opportunistic PPG acquisition during fingerprint authentication on Nexus 5X, and the results may change with other smartphones. In particular, the fingerprint sensor in Nexus 5X is on the backside of the device, designed to be interacted using an index finger. However, other devices have fingerprint sensors on the front side, allowing users to interact with a thumb (e.g., an iPhone). A similar hardware design is conceptually applicable to other devices, but its performance should be carefully re-examined.

This work demonstrates opportunistic PPG sensing in a smartphone, and my demonstration can be extended to other fingerprint authentication scenarios. For instance, a fingerprint sensor installed into an office door can perform PPG sensing when an employee is unlocking it. In such a context, more direct integration of PPG sensing into a fingerprint sensor is possible. However, regardless of user context and sensor architecture, users would steadily hold fingers on top of a sensor. Thus, future work can explore a similar idea to this work in other contexts and my results would offer reference performance information.

My system evaluation did not include patients with heart or cardiovascular disease. Understanding medical implications of extracted cardiovascular features is beyond the scope of this work. I thus do not claim that my sensing technology would offer professional medical recording. Nevertheless, my results revealed that cardiovascular features extracted by the Auth 'n' Scan system can be close to those from the ground truth signals. In addition, my work has demonstrated a potential to extract longer-term features, such as Poincaré plots, from a series of fragmented PPG data if a sufficient number of PPIs are available. This work thus still shows a strong potential of opportunistic PPG sensing during fingerprint authentication.

My work did not include a long-term study on user experience of Auth 'n' Scan. My results found that the sensing duration of five seconds was acceptable though this is still longer than time for unmodified fingerprint authentication. Users might be discouraged to continue to use the Auth 'n' Scan system due to this sensing duration in long-term use. Future work should investigate the user adaptation and experience of Auth 'n' Scan through deployment user studies. The focus of this work primarily lies in the system performance of the current Auth 'n' Scan prototype and demonstration of the feasibility of the dual-purpose biometrics concept in mobile fingerprint authentication.

Chapter 8

Conclusion and Future Work

As the use of biometric authentication is increasing, research can exploit such interaction as a sensing opportunity. I propose a novel security system concept, called dual-purpose biometrics. Dual-purpose biometrics enables concurrent physiological or behavioral sensing during biometric authentication or identification. As an instance of dual-purpose biometrics, I demonstrate Auth 'n' Scan, enabling opportunistic PPG sensing during fingerprint authentication on a smartphone. With my hardware and signal processing algorithm, I achieve heart rate estimation only for five-second sampling if the baseline heart rate of a user is given. My evaluations also show that a feature observed in Poincaré plots, which in general require long sampling of PPIs, can be potentially inferable from a set of fragmented PPG data. Although further improvements on sensing durations and estimation accuracy would increase the viability of the Auth 'n' Scan system, my work well demonstrates the feasibility of concurrent PPG sensing during mobile fingerprint authentication.

As discussed above, future work should investigate how to improve sensing performance as well as user experience of Auth 'n' Scan. Future work should examine how people would use Auth 'n' Scan in their smartphones through a deployment study. Extending Auth 'n' Scan to other fingerprint authentication scenarios is also an interesting future research direction. I believe that this work serves as a foundation for exploration of a broader context of dual-purpose biometrics.

Publications

Publications related to this thesis

Journal

- Takahiro Hashizume, Takuya Arizono, Koji Yatani, "Auth 'n' Scan: Opportunistic Photoplethysmography in Mobile Fingerprint Authentication," In Proceedings of the ACM on Interactive, Mobile, Wearable and Ubiquitous Technologies (IMWUT), vol.1, No.4, Article 137, 27 pages, December 2017.

Patent

- 矢谷浩司，橋爪崇弘，心拍測定装置、心拍測定方法及び心拍測定プログラム，特願 2017-229096，2017/11/29 出願.

国内研究会

- 橋爪崇弘，矢谷浩司，指尖容積脈波を同時に取得する指紋認証システムの試作と評価，第 53 回情報処理学会 UBI 研究会（SIGUBI），Vol.2017-UBI-53，No.56，March 2017，**優秀論文賞受賞**.

Other Publications

International Conference

- Takahiro Hashizume, Takuya Sasatani, Koya Narumi, Yoshiaki Narusue, Yoshihiro Kawahara, Tohru Asami, "Passive and Contactless Epidermal Pressure Sensor Printed with Silver Nano-particle Ink," In Proceedings of the 2016 ACM International Joint Conference on Pervasive and Ubiquitous Computing (UbiComp '16), pp.190–195, Heidelberg, Germany, September 2016.

国内研究会

- 有薗拓也，橋爪崇弘，矢谷浩司，重心移動が可能なダンベル型デバイスの製作とその知覚に関する実験，第 53 回情報処理学会 UBI 研究会（SIGUBI），Vol.2017-UBI-53，No.25，March 2017，**学生奨励賞受賞.**
- 橋爪崇弘，笹谷拓也，成末義哲，川原圭博，浅見徹，銀ナノインクを用いた非接触読み取り可能なパッシブ型静電容量式圧力センサと着圧測定への応用，マルチメディア，分散，協調とモバイルシンポジウム (DICOMO2016)，4G-1，pp.840-845，July 2016，**最優秀論文賞・優秀プレゼンテーション賞受賞.**

国内全国大会

- 松井秀憲，橋爪崇弘，矢谷浩司，氷型スマートデバイス向け光学的アルコール濃度推定手法の調査，情報処理学会全国大会，March 2018, 2V-01, to appear.
- 橋爪崇弘，笹谷拓也，成末義哲，川原圭博，浅見徹，銀ナノインクを用いたパッシブ型圧力センサの人体貼付用途における設計手法，電子情報通信学会総合大会，B-18-17，March 2016.
- 橋爪崇弘，成末義哲，川原圭博，浅見徹，銀ナノインクを用いたパッシブ型静電容量式圧力センサーの試作と評価，電子情報通信学会ソサイエティ大会，B-18-27，September 2015.

国内学会デモ発表

- 有薗拓也，橋爪崇弘，矢谷浩司，筋力トレーニングを指向した Exergame 向け負荷制御の研究，情報処理学会インタラクション，3-6F-06，pp.704–706，March 2017.

References

[1] Rajendra Acharya U, N Kannathal, and S M Krishnan. 2004. Comprehensive analysis of cardiac health using heart rate signals. *Physiological Measurement* 25, 5 (Aug. 2004), 1139–1151. https://doi.org/10.1088/0967-3334/25/5/005

[2] Fadel Adib, Hongzi Mao, Zachary Kabelac, Dina Katabi, and Robert C. Miller. 2015. Smart Homes That Monitor Breathing and Heart Rate. In *Proceedings of the 33rd Annual ACM Conference on Human Factors in Computing Systems (CHI '15)*. ACM, New York, NY, USA, 837–846. https://doi.org/10.1145/2702123.2702200

[3] John Allen. 2007. Photoplethysmography and its application in clinical physiological measurement. *Physiological Measurement* 28, 3 (Feb. 2007), R1–R39. https://doi.org/10.1088/0967-3334/28/3/R01

[4] Heba Aly and Moustafa Youssef. 2016. Zephyr: Ubiquitous Accurate multi-Sensor Fusion-based Respiratory Rate Estimation Using Smartphones. In *Proceedings of the 35th Annual IEEE International Conference on Computer Communications (IEEE INFOCOM '16)*. https://doi.org/10.1109/INFOCOM.2016.7524401

[5] Apple Insider. 2016. Average iPhone user unlocks device 80 times per day, 89% use Touch ID, Apple says. (April 2016). Retrieved January 23, 2018 from http://appleinsider.com/articles/16/04/19/average-iphone-user-unlocks-device-80-times-per-day-89-use-touch-id-apple-says

[6] Rasekhar Bhagavatula, Blase Ur, Kevin Iacovino, Su Mon Kywe, Lorrie Faith Cranor, and Marios Savvides. 2015. Biometric Authentication on iPhone and Android: Usability, Perceptions, and Influences on Adoption. In *Proceedings of the NDSS Workshop on Usable Security (USEC '15)*.

[7] Edward D. Chan, Michael M. Chan, and Mallory M. Chan. 2013. Pulse oximetry: Understanding its basic principles facilitates appreciation of its limitations. *Respiratory Medicine* 107, 6 (June 2013), 789–799. https://doi.org/10.1016/j.rmed.2013.02.004

[8] Hiroshi Chigira, Masayuki Ihara, Minoru Kobayashi, Akimichi Tanaka, and Tomohiro Tanaka. 2014. Heart Rate Monitoring Through the Surface of a Drinkware. In *Proceedings of the 2014 ACM International Joint Conference on Pervasive and Ubiquitous Computing (UbiComp '14)*. ACM, New York, NY, USA, 685–689. https://doi.org/10.1145/2632048.2632101

[9] Alexander De Luca, Alina Hang, Emanuel von Zezschwitz, and Heinrich Hussmann. 2015. I Feel Like I'm Taking Selfies All Day!: Towards Understanding Biometric

Authentication on Smartphones. In *Proceedings of the 33rd Annual ACM Conference on Human Factors in Computing Systems (CHI '15)*. ACM, New York, NY, USA, 1411–1414. https://doi.org/10.1145/2702123.2702141

[10] Anind K. Dey, Katarzyna Wac, Denzil Ferreira, Kevin Tassini, Jin-Hyuk Hong, and Julian Ramos. 2011. Getting Closer: An Empirical Investigation of the Proximity of User to Their Smart Phones. In *Proceedings of the 13th International Conference on Ubiquitous Computing (UbiComp '11)*. ACM, New York, NY, USA, 163–172. https://doi.org/10.1145/2030112.2030135

[11] Rachel Eardley, Anne Roudaut, Steve Gill, and Stephen J. Thompson. 2017. Understanding Grip Shifts: How Form Factors Impact Hand Movements on Mobile Phones. In *Proceedings of the 2017 CHI Conference on Human Factors in Computing Systems (CHI '17)*. ACM, New York, NY, USA, 4680–4691. https://doi.org/10.1145/3025453.3025835

[12] Mohamed Elgendi. 2012. On the Analysis of Fingertip Photoplethysmogram Signals. *Current Cardiology Reviews* 8, 1 (2012), 14–25. https://doi.org/10.2174/157340312801215782

[13] Biyi Fang, Nicholas D. Lane, Mi Zhang, Aidan Boran, and Fahim Kawsar. 2016. BodyScan: Enabling Radio-based Sensing on Wearable Devices for Contactless Activity and Vital Sign Monitoring. In *Proceedings of the 14th Annual International Conference on Mobile Systems, Applications, and Services (MobiSys '16)*. ACM, New York, NY, USA, 97–110. https://doi.org/10.1145/2906388.2906411

[14] FIDO Alliance Inc. 2012. FIDO Alliance. (July 2012). Retrieved January 23, 2018 from https://fidoalliance.org/

[15] Erin Griffiths, T. Scott Saponas, and A. J. Bernheim Brush. 2014. Health Chair: Implicitly Sensing Heart and Respiratory Rate. In *Proceedings of the 2014 ACM International Joint Conference on Pervasive and Ubiquitous Computing (UbiComp '14)*. ACM, New York, NY, USA, 661–671. https://doi.org/10.1145/2632048.2632099

[16] Mehrdad Hessar, Vikram Iyer, and Shyamnath Gollakota. 2016. Enabling On-body Transmissions with Commodity Devices. In *Proceedings of the 2016 ACM International Joint Conference on Pervasive and Ubiquitous Computing (UbiComp '16)*. ACM, New York, NY, USA, 1100–1111. https://doi.org/10.1145/2971648.2971682

[17] Christian Holz and Patrick Baudisch. 2010. The Generalized Perceived Input Point Model and How to Double Touch Accuracy by Extracting Fingerprints. In *Proceedings of the SIGCHI Conference on Human Factors in Computing Systems (CHI '10)*. ACM, New York, NY, USA, 581–590. https://doi.org/10.1145/1753326.1753413

[18] Christian Holz and Patrick Baudisch. 2013. Fiberio: A Touchscreen That Senses Fingerprints. In *Proceedings of the 26th Annual ACM Symposium on User Interface Software and Technology (UIST '13)*. ACM, New York, NY, USA, 41–50. https://doi.org/10.1145/2501988.2502021

[19] Christian Holz and Frank R. Bentley. 2016. On-Demand Biometrics: Fast Cross-Device Authentication. In *Proceedings of the 2016 CHI Conference on Human Factors in Computing Systems (CHI '16)*. ACM, New York, NY, USA, 3761–3766. https://doi.org/10.1145/2858036.2858139

[20] Christian Holz and Edward J. Wang. 2017. Glabella: Continuously Sensing Blood Pressure Behavior Using an Unobtrusive Wearable Device. *Proceedings of the ACM on Interactive, Mobile, Wearable and Ubiquitous Technologies* 1, 3, Article 58 (Sept. 2017), 23 pages. https://doi.org/10.1145/3132024

[21] Gary Hsieh, Ian Li, Anind Dey, Jodi Forlizzi, and Scott E. Hudson. 2008. Using Visualizations to Increase Compliance in Experience Sampling. In *Proceedings of the 10th International Conference on Ubiquitous Computing (UbiComp '08)*. ACM, New York, NY, USA, 164–167. https://doi.org/10.1145/1409635.1409657

[22] Anil K. Jain, Jianjiang Feng, and Karthik Nandakumar. 2010. Fingerprint Matching. *Computer* 43, 2 (Feb. 2010), 36–44. https://doi.org/10.1109/MC.2010.38

[23] P. W. Kamen and A. M. Tonkin. 1995. Application of the Poincaré plot to heart rate variability: a new measure of functional status in heart failure. *Australian and New Zealand Journal of Medicine* 25, 1 (1995), 18–26. https://doi.org/10.1111/j.1445-5994.1995.tb00573.x

[24] Seungwoo Kang, Sungjun Kwon, Chungkuk Yoo, Sangwon Seo, Kwangsuk Park, Junehwa Song, and Youngki Lee. 2014. Sinabro: Opportunistic and Unobtrusive Mobile Electrocardiogram Monitoring System. In *Proceedings of the 15th Workshop on Mobile Computing Systems and Applications (HotMobile '14)*. ACM, New York, NY, USA, Article 11, 6 pages. https://doi.org/10.1145/2565585.2565605

[25] Amy K Karlson, Benjamin B Bederson, and Jose L Contreras-Vidal. 2008. Understanding one-handed use of mobile devices. In *Handbook of Research on User Interface Design and Evaluation for Mobile Technology*, Joanna Lumsden (Ed.). IGI Global, Hershey, PA, 86–101. https://doi.org/10.4018/978-1-59904-871-0.ch006

[26] Ilkka Korhonen, Juha Pärkkä, and Mark van Gils. 2003. Health monitoring in the home of the future. *IEEE Engineering in Medicine and Biology Magazine* 22, 3 (2003), 66–73. https://doi.org/10.1109/MEMB.2003.1213628

[27] Jennifer R. Kwapisz, Gary M. Weiss, and Samuel A. Moore. 2011. Activity Recognition using Cell Phone Accelerometers. *ACM SIGKDD Explorations Newsletter* 12, 2 (March 2011), 74–82. https://doi.org/10.1145/1964897.1964918

[28] Kristof van Laerhoven, Marko Borazio, and Jan Hendrik Burdinski. 2015. Wear is Your Mobile? Investigating Phone Carrying and Use Habits with a Wearable Device. *Frontiers in ICT* 2, Article 10 (May 2015), 10 pages. https://doi.org/10.3389/fict.2015.00010

[29] Reham Mohamed and Moustafa Youssef. 2017. HeartSense: Ubiquitous Accurate Multi-Modal Fusion-based Heart Rate Estimation Using Smartphones. *Proceedings of the ACM on Interactive, Mobile, Wearable and Ubiquitous Technologies* 1, 3, Article 97 (Sept. 2017), 18 pages. https://doi.org/10.1145/3132028

[30] Joel Murphy and Yury Gitman. 2011. Open Hardware - World Famous Electronics llc. (2011). Retrieved January 23, 2018 from http://pulsesensor.com/pages/open-hardware

[31] Martin Pielot, Tilman Dingler, Jose San Pedro, and Nuria Oliver. 2015. When Attention is Not Scarce - Detecting Boredom from Mobile Phone Usage. In *Proceedings of the 2015 ACM International Joint Conference on Pervasive and Ubiquitous Computing (UbiComp '15)*. ACM, New York, NY, USA, 825–836. https://doi.org/10.1145/2750858.2804252

[32] Ming-Zher Poh, Kyunghee Kim, Andrew D. Goessling, Nicholas C. Swenson, and Rosalind W. Picard. 2012. Cardiovascular Monitoring Using Earphones and a Mobile Device. *IEEE Pervasive Computing* 11, 4 (Oct. 2012), 18–26. https://doi.org/10.1109/MPRV.2010.91

[33] Ming-Zher Poh, Daniel McDuff, and Rosalind W. Picard. 2011. A Medical Mirror for Non-contact Health Monitoring. In *ACM SIGGRAPH 2011 Emerging Technologies (SIGGRAPH '11)*. ACM, New York, NY, USA, Article 2, 1 pages. https://doi.org/10.1145/2048259.2048261

[34] Lunji Qiu. 2014. Fingerprint sensor technology. In *Proceedings of the 9th IEEE Conference on Industrial Electronics and Applications (ICIEA '14)*. IEEE, 1433–1436. https://doi.org/10.1109/ICIEA.2014.6931393

[35] Nalini K. Ratha, Jonathan H. Connell, and Ruud M. Bolle. 2001. Enhancing security and privacy in biometrics-based authentication systems. *IBM Systems Journal* 40, 3 (2001), 614–634. https://doi.org/10.1147/sj.403.0614

[36] Arun Ross and Anil K. Jain. 2004. Multimodal biometrics: An overview. In *Proceedings of the 12th European Signal Processing Conference (EUSIPCO '04)*. IEEE, 1221–1224.

[37] Masoud Rostami, Ari Juels, and Farinaz Koushanfar. 2013. Heart-to-heart (H2H): authentication for implanted medical devices. In *Proceedings of the 2013 ACM SIGSAC conference on Computer & communications security (CCS '13)*. ACM, New York, NY, USA, 1099–1112. https://doi.org/10.1145/2508859.2516658

[38] Stefan Sammito, Wiebke Sammito, and Irina Böckelmann. 2016. The circadian rhythm of heart rate variability. *Biological Rhythm Research* 47, 5 (May 2016), 717–730. https://doi.org/10.1080/09291016.2016.1183887

[39] M. Angela Sasse and Ivan Flechais. 2005. Usable security: Why do we need it? How do we get it? In *Security and Usability : Designing Secure Systems that People Can Use*, Lorrie Faith Cranor and Simson Garfinkel (Eds.). O'Reilly, Chapter 2, 13–30.

[40] Felix Scholkmann, Jens Boss, and Martin Wolf. 2012. An Efficient Algorithm for Automatic Peak Detection in Noisy Periodic and Quasi-Periodic Signals. *Algorithms* 5, 4 (Nov. 2012), 588–603. https://doi.org/10.3390/a5040588

[41] N. Selvaraj, A. Jaryal, J. Santhosh, K. K. Deepak, and S. Anand. 2008. Assessment of heart rate variability derived from finger-tip photoplethysmography as compared to electrocardiography. *Journal of Medical Engineering & Technology* 32, 6 (July 2008), 479–484. https://doi.org/10.1080/03091900701781317

[42] Dale R. Setlak. 2004. Advances in Fingerprint Sensors Using RF Imaging Techniques. In *Automatic Fingerprint Recognition Systems*, Nalini Ratha and Ruud Bolle (Eds.). Springer, New York, NY, 27–53. https://doi.org/10.1007/0-387-21685-5_2

[43] Mridula Singh, Abhishek Kumar, Kuldeep Yadav, Himanshu Madhu, and Tridib Mukherjee. 2015. Mauka-mauka: Measuring and Predicting Opportunities for Webcam-based Heart Rate Sensing in Workplace Environment. In *Proceedings of the 10th EAI International Conference on Body Area Networks (BodyNets '15)*. ICST, Brussels, Belgium, 96–102. https://doi.org/10.4108/eai.28-9-2015.2261492

[44] Atsushi Sugiura and Yoshiyuki Koseki. 1998. A User Interface Using Fingerprint Recognition: Holding Commands and Data Objects on Fingers. In *Proceedings of the 11th Annual ACM Symposium on User Interface Software and Technology (UIST '98)*. ACM, New York, NY, USA, 71–79. https://doi.org/10.1145/288392.288575

[45] Khai N. Truong, Thariq Shihipar, and Daniel J. Wigdor. 2014. Slide to X: Unlocking the Potential of Smartphone Unlocking. In *Proceedings of the 32nd Annual ACM Conference on Human Factors in Computing Systems (CHI '14)*. ACM, New York, NY, USA, 3635–3644. https://doi.org/10.1145/2556288.2557044

[46] Rajan Vaish, Keith Wyngarden, Jingshu Chen, Brandon Cheung, and Michael S. Bernstein. 2014. Twitch Crowdsourcing: Crowd Contributions in Short Bursts of Time. In *Proceedings of the 32nd Annual ACM Conference on Human Factors in Computing Systems (CHI '14)*. ACM, New York, NY, USA, 3645–3654. https://doi.org/10.1145/2556288.2556996

[47] Hao-Yu Wu, Michael Rubinstein, Eugene Shih, John Guttag, Frédo Durand, and William Freeman. 2012. Eulerian Video Magnification for Revealing Subtle Changes in the World. *ACM Transactions on Graphics* 31, 4, Article 65 (July 2012), 8 pages. https://doi.org/10.1145/2185520.2185561

[48] Takahiro Yoshizaki, Yukari Kawano, Yuki Tada, Azumi Hida, Toru Midorikawa, Kohe Hasegawa, Takeshi Mitani, Taiki Komatsu, and Togo Fumiharu. 2013. Diurnal 24-Hour Rhythm in Ambulatory Heart Rate Variability during the Day Shift in Rotating Shift Workers. *Journal of Biological Rhythms* 28, 3 (June 2013), 227–236. https://doi.org/10.1177/0748730413489957